The Plant Cell, Vol. 21: 892–909, March 2009, www.plantcell.org

A Chloroplastic UDP-Glucose Pyrophosphorylase from *Arabidopsis* Is the Committed Enzyme for the First Step of Sulfolipid Biosynthesis [W][OA]

Yozo Okazaki,[a] Mie Shimojima,[b,c] Yuji Sawada,[a,d] Kiminori Toyooka,[a] Tomoko Narisawa,[a] Keiichi Mochida,[a] Hironori Tanaka,[b] Fumio Matsuda,[a] Akiko Hirai,[a] Masami Yokota Hirai,[a,d] Hiroyuki Ohta,[c,e] and Kazuki Saito[a,f,1]

[a] RIKEN Plant Science Center, Tsurumi-ku, Yokohama 230-0045, Japan
[b] Graduate School of Bioscience and Biotechnology, Tokyo Institute of Technology, Midori-ku, Yokohama 226-8501, Japan
[c] Research Center for the Evolving Earth and Planets, Tokyo Institute of Technology, Midori-ku, Yokohama 226-8501, Japan
[d] Japan Science and Technology Agency, Core Research for Evolutional Science and Technology, Kawaguchi, 332-0012, Japan
[e] Center for Biological Resources and Informatics, Tokyo Institute of Technology, Midori-ku, Yokohama 226-8501, Japan
[f] Graduate School of Pharmaceutical Sciences, Chiba University, Inage-ku, Chiba 263-8522, Japan

Plants synthesize a sulfur-containing lipid, sulfoquinovosyldiacylglycerol, which is one of three nonphosphorus glycerolipids that provide the bulk of the structural lipids in photosynthetic membranes. Here, the identification of a novel gene, *UDP-glucose pyrophosphorylase3* (*UGP3*), required for sulfolipid biosynthesis is described. Transcriptome coexpression analysis demonstrated highly correlated expression of *UGP3* with known genes for sulfolipid biosynthesis in *Arabidopsis thaliana*. Liquid chromatography–mass spectrometry analysis of leaf lipids in two *Arabidopsis ugp3* mutants revealed that no sulfolipid was accumulated in these mutants, indicating the participation of *UGP3* in sulfolipid biosynthesis. From the deduced amino acid sequence, UGP3 was presumed to be a UDP-glucose pyrophosphorylase (UGPase) involved in the generation of UDP-glucose, serving as the precursor of the polar head of sulfolipid. Recombinant UGP3 was able to catalyze the formation of UDP-glucose from glucose-1-phosphate and UTP. A transient assay using fluorescence fusion proteins and UGPase activity in isolated chloroplasts indicated chloroplastic localization of UGP3. The transcription level of *UGP3* was increased by phosphate starvation. A comparative genomics study on *UGP3* homologs across different plant species suggested the structural and functional conservation of the proteins and, thus, a committing role for UGP3 in sulfolipid synthesis.

INTRODUCTION

The photosynthetic membranes of plants are rich in nonphosphorus glycolipids, including galactolipids, mono- and digalactosyldiacylglycerol (MGDG and DGDG), and sulfolipid, sulfoquinovosyldiacylglycerol (SQDG). SQDG is a lipid class that has a unique polar-head constituent, sulfoquinovose, a derivative of glucose in which the 6-hydroxy is replaced by a sulfonate group. SQDG is widely distributed among photosynthetic organisms such as bacteria, cyanobacteria, algae, mosses, ferns, and higher plants (Haines, 1973). The exact role of SQDG under normal growth conditions is still obscure. Mutants of photosynthetic bacteria, *Arabidopsis thaliana*, and *Chlamydomonas reinhardtii* completely lacking this lipid show only subtle impairments in photosynthesis and growth unless they are phosphate starved (Benning et al., 1993; Güler et al., 1996; Yu et al., 2002; Riekhof et al., 2003). In photosynthetic organisms, the relative amount of total anionic thylakoid lipids is typically maintained by reciprocally adjusting the contents of SQDG and phosphatidylglycerol (PG) as phosphate availability changes. Typically, the relative content of PG decreases and that of SQDG increases following phosphate limitation (Essigmann et al., 1998; Härtel et al., 2000; Yu et al., 2002). In SQDG-deficient mutants, the proportion of PG does not decrease under phosphate limitation, and these mutants become phosphate starved sooner than their respective wild types (Benning et al., 1993; Güler et al., 1996; Yu et al., 2002; Riekhof et al., 2003). These observations suggest that one of the main functions of SQDG is to substitute for PG under phosphate limitation to maintain the proper balance of anionic charge in the thylakoid membrane (Benning et al., 1993; Güler et al., 1996; Yu et al., 2002, 2003). Recently, SQDG was reported to be used as a significant internal sulfur source for protein biosynthesis in an early phase of sulfur starvation in *C. reinhardtii* (Sugimoto et al., 2007). SQDG is one of the primary sulfur-containing organic compounds in higher plants, but it remains unclear whether it plays the same role in higher plants as observed in *C. reinhardtii*.

In *Arabidopsis*, SQDG is synthesized in two unique steps (Figure 1): the assembly of UDP-glucose (UDP-Glc) and sulfite into UDP-sulfoquinovose (UDP-SQ) by UDP-sulfoquinovose

[1] Address correspondence to ksaito@psc.riken.jp.
The author responsible for distribution of materials integral to the findings presented in this article in accordance with the policy described in the Instructions for Authors (www.plantcell.org) is: Kazuki Saito (ksaito@psc.riken.jp).
[W]Online version contains Web-only data.
[OA]Open Access articles can be viewed online without a subscription.
www.plantcell.org/cgi/doi/10.1105/tpc.108.063925

synthase SQD1 (Essigmann et al., 1998; Sanda et al., 2001), and the subsequent transfer of sulfoquinovose from UDP-SQ to diacylglycerol for synthesis of the final product by SQDG synthase SQD2 (Yu et al., 2002). These two specific reactions have been determined to occur in chloroplasts based on feeding experiments of isolated chloroplasts with ^{35}S-labeled sulfate, which revealed that chloroplasts were fully capable of synthesizing SQDG from labeled sulfate (Haas et al., 1980; Kleppinger-Sparace et al., 1985; Joyard et al., 1986; Kleppinger-Sparace and Mudd, 1987, 1990; Pugh et al., 1995) and based on enzyme activities of SQD1 and SQD2 in the chloroplasts (Heinz et al., 1989; Seifert and Heinz, 1992; Tietje and Heinz, 1998; Shimojima et al., 2005). Recombinant SQD1 proteins have been shown to have UDP-SQ synthase activity (Essigmann et al., 1998; Shimojima and Benning, 2003), and the crystal structure of the *Arabidopsis* SQD1 protein and detailed possible reaction mechanism have been reported (Mulichak et al., 1999; Essigmann et al., 1999). In addition, analysis of SQD1 purified from leaves of spinach (*Spinacia oleracea*) suggested that native SQD1 interacted with ferredoxin-dependent glutamate synthase to form a large protein complex in the stroma of plants (Shimojima et al., 2005).

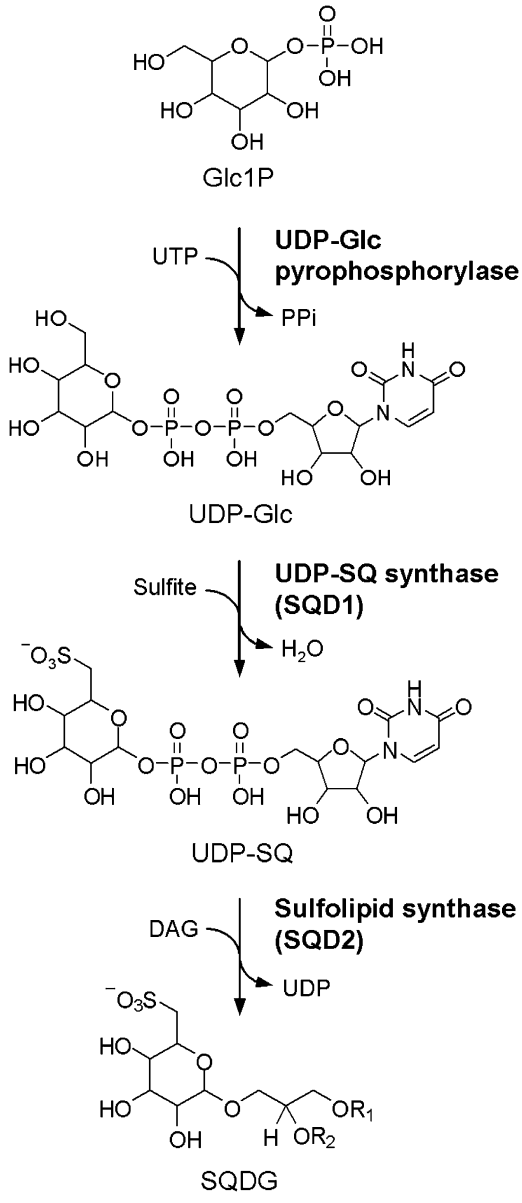

Figure 1. The Sulfolipid Biosynthesis Pathway in *Arabidopsis*.

Three enzymes involved in sulfolipid biosynthesis are indicated. *SQD1* and *SQD2* have already been identified (Essigmann et al., 1998; Yu et al., 2002). UTP, uridine-5′-triphosphate; PPi, pyrophosphate; DAG, 1,2-diacylglycerol; R, fatty acid group.

Although SQD1 and SQD2 have been characterized at genetic and enzymatic levels, the mechanism of supply of UDP-Glc for the SQDG biosynthetic pathway remains to be addressed. In plants, SQD1 is localized in the stroma of chloroplasts and uses UDP-Glc as a substrate, raising the question of the source of the UDP-Glc. The concentration of UDP-Glc in the chloroplasts is considered to be very low (Bligny et al., 1990). There have been two models developed as possible answers to this question: (1) UDP-Glc is imported into the chloroplasts from the cytosol; (2) UDP-Glc is generated inside the chloroplasts (Benning, 2007).

Along with the massive accumulation of microarray data sets, transcriptome coexpression analysis has proven to be a powerful tool for identifying regulatory relationships in the transcriptional networks of model organisms, including *Escherichia coli* (Balázsi et al., 2005) and yeast (Ihmels et al., 2004). A set of genes involved in a particular biological process (more practically, in a particular metabolic pathway) are often coexpressed under the control of a shared regulatory system. Therefore, if an unknown gene is coexpressed with known genes of a particular metabolic pathway, this unknown gene is probably involved in the pathway (Saito et al., 2008). Based on this concept, new metabolic genes have been identified in *Arabidopsis* by transcriptome coexpression analysis (Persson et al., 2005; Tohge et al., 2005; Yonekura-Sakakibara et al., 2007, 2008; Hirai et al., 2007).

In this study, a novel gene involved in SQDG biosynthesis in *Arabidopsis* was identified. Using transcriptome coexpression analysis, we prioritized a previously uncharacterized gene highly coexpressed with known SQDG biosynthetic genes. Lipid profiling of knockout mutants of this gene and an enzyme assay for recombinant protein confirmed that this gene encodes UDP-glucose pyrophosphorylase (UGPase) involved in the supply of UDP-Glc to the chloroplasts requisite for SQDG biosynthesis. The mechanism, regulation, and evolution of SQDG biosynthesis were further clarified.

RESULTS

An Uncharacterized Gene *UGP3* (At3g56040) Is Highly Coexpressed with Genes Involved in SQDG Biosynthesis

To identify novel genes involved in lipid metabolism, coexpression analyses were conducted within the ATTED-II database using a coexpression gene search program on the RIKEN PRIMe website (Obayashi et al., 2007; Akiyama et al., 2008). Based on

the concept that a set of genes involved in a biological process are coregulated under the control of a shared regulatory system, the coexpression pattern of genes involved in the metabolism of polar glycerolipids in plastids was analyzed. Coexpression relationships are visualized as a graph, in which a pair of genes (two vertices) with a high correlation coefficient (>0.50) is connected by a line (Figure 2). Four known genes (*SQD1*, *SQD2*, *MGD2*, and *MGD3*) involved in sulfolipid and galactolipid biosynthetic pathways are clustered in the same group, suggesting a shared regulatory system for these pathways. Genes that coexpressed with at least two of these four genes were selected based on their correlation coefficient (>0.50 with all conditions), considering annotations for gene functions. These analyses revealed that an unknown gene, At3g56040, and two genes coding putative lipases (At1g08310 and At2g42690) were coexpressed with *SQD1*, *SQD2*, *MGD2*, and *MGD3* (Figure 2), suggesting the involvement of these genes in the biosynthesis of SQDG or galactolipid. In particular, At3g56040, coexpressing with *SQD1* and *SQD2*, was predicted to be involved in SQDG synthesis, although this gene is annotated only as a gene coding an expressed protein. From this point, this gene will be referred to as *UGP3*, since in the following sections the product of this gene is demonstrated to exhibit UGPase activity, and two UGPase genes, *UGP1* and *UGP2*, have been reported previously (Meng et al., 2008). The prediction that *UGP3* was involved in SQDG biosynthesis was reinforced by examining the tissue-specific expression patterns of transcripts of *UGP3*, *SQD1*, and *SQD2*; *Arabidopsis* eFP-Browser (Winter et al., 2007) showed that these three genes are coordinately expressed in leaves, stems, and flowers (see Supplemental Figure 1 online), thus supporting the close relationship among these genes. The transcript levels of *UGP3* were upregulated by phosphate limitation, as reported for *SQD1* and *SQD2* (Essigmann et al., 1998; Yu et al., 2002), as shown by an analysis using Genevestigator (Zimmermann et al., 2005) (see Supplemental Figure 2 online). These results of gene expression analyses support the hypothesis that *UGP3* is involved in SQDG biosynthesis.

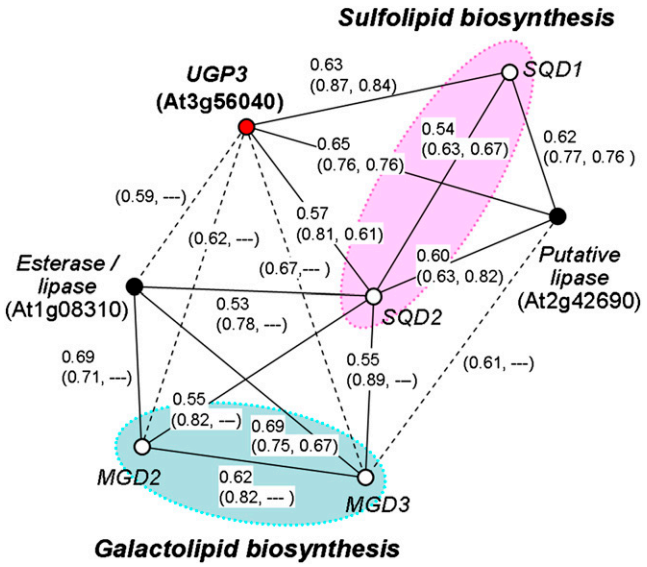

Figure 2. Transcriptome Coexpression Analysis of the Genes Involved in Polar Glycerolipid Biosynthesis in Chloroplasts.

Open circles indicate genes whose physiological functions are known. The closed circle colored in red indicates *UGP3*, and closed circles colored in black indicate genes whose functions have not been identified. Ovals indicate the gene groups that are involved in particular metabolic pathways: the pink one indicates sulfolipid biosynthetic genes, and the blue one indicates galactolipid biosynthetic genes. Positive correlations ($r > 0.50$) in all data sets (tissue and development, stress treatments, and hormone treatments) are indicated with connecting lines (r, Pearson's correlation coefficient). The lengths of the lines and the distances between circles are valueless. Correlations that were only observed in particular data sets were also analyzed. Positive correlations ($r > 0.50$) observed only in the hormone treatment data set or the tissue and development data set are represented by broken lines. The r values calculated from all data sets are shown along the connecting line, and those of the hormone treatment and tissue and development data sets are shown in parentheses. When the r value for the hormone treatment and tissue and development data sets is smaller than 0.5, "---" is shown instead of the actual r value.

Two *ugp3* Mutants Are Completely Devoid of SQDG

To examine the function of *UGP3* in vivo, two independent T-DNA insertion lines obtained from the SALK collection were investigated (Alonso et al., 2003). Sequence analysis of the flanking regions of the T-DNA revealed that the T-DNA insertion sites of SALK_020654 (designated as *ugp3-1*) and SALK_073806 (designated as *ugp3-2*) were located in exon 1 (75 bp downstream from the ATG) and exon 15 (4340 bp downstream from the ATG), respectively (see Supplemental Figure 3A online). No transcripts of *UGP3* were detected using RT-PCR in the homozygotes of either mutant line (see Supplemental Figure 3B online), and there were no obvious phenotypic abnormalities in the mutant plants.

Crude lipid fractions were extracted from the rosette leaves of wild-type plants and two *ugp3* mutants and subjected to liquid chromatography/ion trap time-of-flight mass spectrometry (LC-IT-TOF-MS). Chromatographic separations were performed using hydrophilic interaction chromatography based on the interactions between the polar moieties of the stationary phase and the analytes. Thus, the separation mode is almost same as that of normal phase chromatography on silica gels, and lipid molecules were separated based on their polar moieties. The major SQDG species in the leaves of wild-type *Arabidopsis* observed with negative electrospray ionization (ESI)-MS were the same as reported previously (Welti et al., 2003) (see Supplemental Figure 4A online). The structure of the polar headgroup was also confirmed by MS/MS spectra that displayed the ions specific to sulfoquinovose moiety as reported (Welti et al., 2003) (see Supplemental Figures 4B and 4C online). Based on these data, the accumulation patterns of SQDG in the leaves of wild-type plants and two *ugp3* mutants were analyzed by comparing the intensities of the extracted ion chromatograms of the $[M\text{-}H]^-$ species of SQDG (see Supplemental Figure 5 online). No accumulation of SQDG was observed in either the *ugp3-1* or *ugp3-2* mutant. These results indicate that SQDG biosynthesis was completely inactivated in the two *ugp3* mutants. Profiles of polar glycerolipids, including SQDG, were compared for lipid extracts

from leaves of wild-type plants and *ugp3* mutants (Figure 3). No remarkable changes in the amounts of specific lipid species were observed except for SQDG, although slight but statistically significant increases in several molecular species of PG (34:3 and 34:4 PG) and phosphatidylinositol (34:3 PI) were observed. To investigate wide-ranging alteration of metabolites, untargeted analyses using LC-IT-TOF-MS for other lipids and using ultra-performance liquid chromatography (UPLC)-Q-TOF-MS for more general hydrophilic metabolites were also performed. However, no significant changes were observed except in the amounts of SQDG, indicating the specific involvement of UGP3 in SQDG biosynthesis (see Supplemental Figures 6 and 7 online).

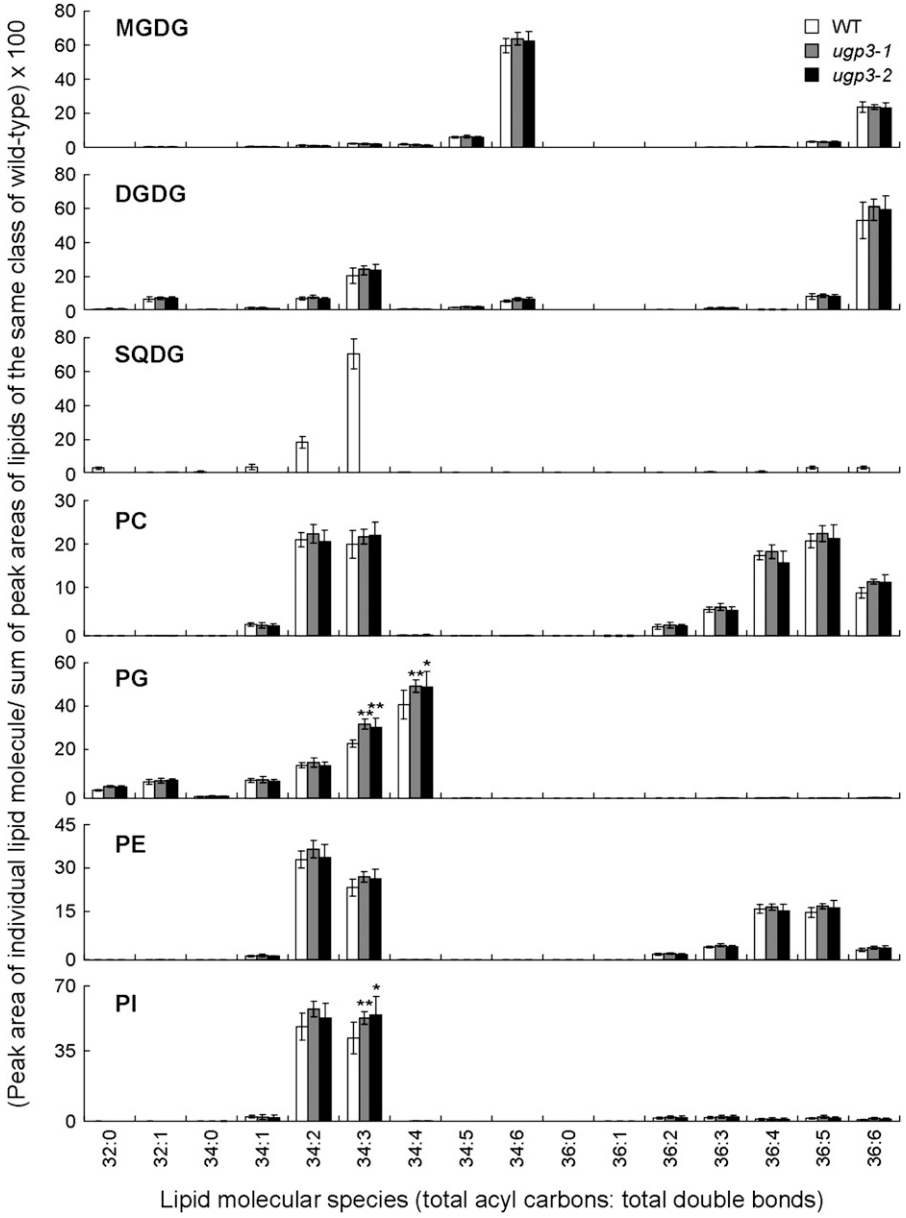

Figure 3. Profiles of Polar Glycerolipids in Leaves of the Wild Type and *ugp3* Mutants.

Peak areas of individual lipid molecules were determined by monitoring their molecular-related ions or fragment ions (see Methods). Levels of individual lipid molecules in the wild type and mutant lines were expressed as relative values against the sum of the peak areas of lipid molecules with the same polar headgroups in the wild type. For example, in the case of 34:6 MGDG in *ugp3-1*, {(peak area of 34:6 MGDG molecule in 34:6 MGDG)/(total area of all MGDG species in the wild type)}*100 was expressed as the height of the bar. Each data point expresses the mean of eight experiments ± SD. Asterisks indicate a statistically significant difference from the wild type (*P < 0.05, **P < 0.01, Student's *t* test). PC, phosphatidylcholine; PE, phosphatidylethanolamine.

Analysis of the Amino Acid Sequence of UGP3 Suggests That *UGP3* Encodes UGPase

The protein corresponding to the *UGP3* gene contains 883 amino acids and a predicted chloroplast-targeting peptide of 72 amino acids at the N-terminus (ChloroP; Emanuelsson et al., 1999), thereby suggesting that the UGP3 protein is localized in the chloroplasts. The amino acid sequence of UGP3 has a homology with those of grape (*Vitis vinifera*) (GSVIVP00029334001), rice (*Oryza sativa*) (Os05g0468600), *C. reinhardtii* (AAY31019, LPB1), *Ostreococcus tauri* (CAL56361), and the gram-negative bacterium *Candidatus Protochlamydia amoebophila* UWE25 (YP_007323) previously referred to as *Parachlamydia*-related strain UWE25, with an identity of 64, 54, 45, 45, and 39%, respectively, forming a distinct subfamily (Figure 4A; see Supplemental Figure 8 online). All of these proteins are annotated as unknown proteins except LPB1 from *C. reinhardtii*. The *lpb1* mutant of *C. reinhardtii* was reported to die more rapidly than the wild type during phosphorus and sulfur limitation (Chang et al., 2005), but its function has not been determined at a biochemical level. The sequence of UGP3 also shares low but significant identities with UDP-sugar pyrophosphorylase (USPase) from *Cucumis melo* (ABD59006; 22%) and *Pisum sativum* (Q5W915; 22%), which accept a wide range of hexose 1-phosphates as substrates, at the amino acid level. The polypeptide of UGP3 contains a putative pyrophosphorylase consensus motif and a nucleotide binding motif (Figure 4B). These structural features of the protein sequence suggest that the UGP3 protein is a chloroplast-localized UGPase for the generation of UDP-Glc from glucose-1-phosphate and UTP. As shown in Figure 4A, the proteins categorized in the subfamily containing UGP3, provisionally designated as type B UGPases, are distinct from the previously characterized subfamilies UDP-*N*-acetylglucosamine pyrophosphorylases, USPases, and another type of UGPases provisionally donated as type A UGPases, consisting of many reported UGPases.

Recombinant UGP3 Exhibits UGPase Activity

Recombinant UGP3 protein, which lacks putative chloroplastic transit peptides (72 residues) at the N-terminus, was expressed in *E. coli* (see Supplemental Figure 9 online). UGPase activity was examined for the forward reaction (synthesis of UDP-Glc). The enzyme reaction product was subjected to UPLC-Q-MS analysis. The recombinant UGP3 protein catalyzed the formation of UDP-Glc from [1-^{13}C]glucose-1-phosphate (Glc1P) and UTP, as confirmed by comparing its chromatographic behavior on liquid chromatography and its mass spectrum with those of the standard compound (Figure 5; see Supplemental Figure 10 online). The molecular weight of the enzyme product was larger than that of standard unlabeled UDP-Glc by one mass unit, while the mass-to-charge (*m/z*) value of the fragment ion attributable to UMP did not change (see Supplemental Figure 10 online). These are reasonable results if the one enriched ^{13}C in Glc1P was successively incorporated into the glucose moiety of UDP-Glc. The specificity of UGP3 for the acceptor of the uridyl group was examined using various kinds of hexose monophosphates in the presence of UTP (Table 1). The enzyme activity of the recombinant UGP3 exhibited a highest specificity for Glc1P, followed by galactose-1-phosphate (Gal1P). No uridyltransferase activity was detected for other hexose monophosphates. The specificity of the recombinant UGP3 for nucleotide triphosphates was also examined using UTP, ATP, CTP, and GTP in the presence of [1-^{13}C]Glc1P. Among the tested compounds, only UTP served as a substrate for UGP3. The K_m values of the recombinant UGP3 for Glc1P and UTP, which were determined to be 0.24 and 0.031 mM, respectively, were similar with those of reported USPases from pea and *Arabidopsis* (Kotake et al., 2004, 2007; Litterer et al., 2006).

Many UDP-hexose pyrophosphorylases have been reported to require the divalent cation Mg^{2+} for activity. To examine its requirement for Mg^{2+} for activity, the UGPase activity of UGP3 was measured at various concentrations of Mg^{2+} (0.1 to 30 mM). The enzyme showed an absolute requirement for the divalent cation Mg^{2+} for activity (Table 2). Enzyme activity was found to be almost equilibrated in the range of 5 to 10 mM of Mg^{2+}. These results are consistent with previous studies on UGPases from humans, *Acanthamoeba castellanii*, and potato (*Solanum tuberosum*) (Tsuboi et al., 1969; Rudick and Weisman, 1974; Nakano et al., 1989) and USPases from pea and *Arabidopsis* (Kotake et al., 2004, 2007), in which the MgUTP complex was postulated to be the actual substrate for the UGPases. The effect of pyrophosphate on the UGPase activity of the recombinant UGP3 was examined. Addition of pyrophosphate strongly inhibited the UGPase activity of the recombinant UGP3 (Table 3), as has been reported for other UGPases and USPases (Tsuboi et al., 1969; Rudick and Weisman, 1974; Nakano et al., 1989; Kotake et al., 2004, 2007) because of the product inhibition mechanism.

UGP3 Is Located in the Chloroplasts

To confirm the chloroplastic targeting of UGP3, the N-terminal 200 amino acids, including the predicted chloroplastic transit peptide (cTP) of UGP3, were fused to the yellow fluorescent protein (YFP) reporter gene (Figure 6A) and subsequently used to transiently transform *Arabidopsis* cells. Figure 6B shows that the fluorescence derived from YFP was associated with the chloroplasts, which were identified by the red autofluorescence of their chlorophylls. Transient expression of SQD1 and UGP3, which were C-terminally fused with the green fluorescence protein (GFP) reporter gene in onion epidermal cells, also showed that both SQD1 and UGP3 were targeted to the plastids (see Supplemental Figure 11 online). These two experiments indicate that UGP3 is a chloroplast-localized protein.

UGPase Activity Is Severely Diminished in Chloroplasts in *ugp3* Mutants

Intact chloroplasts were isolated from leaves of wild-type plants and *ugp3* mutants, and the UGPase activity in isolated chloroplasts was measured (see Supplemental Figure 12 online). A severe decrease (~50%) in UGPase activity was observed in chloroplasts from the *ugp3* mutants compared with the wild type, suggesting that UGP3 is responsible for a majority of the UGPase activity in chloroplasts. However, substantial activity was still

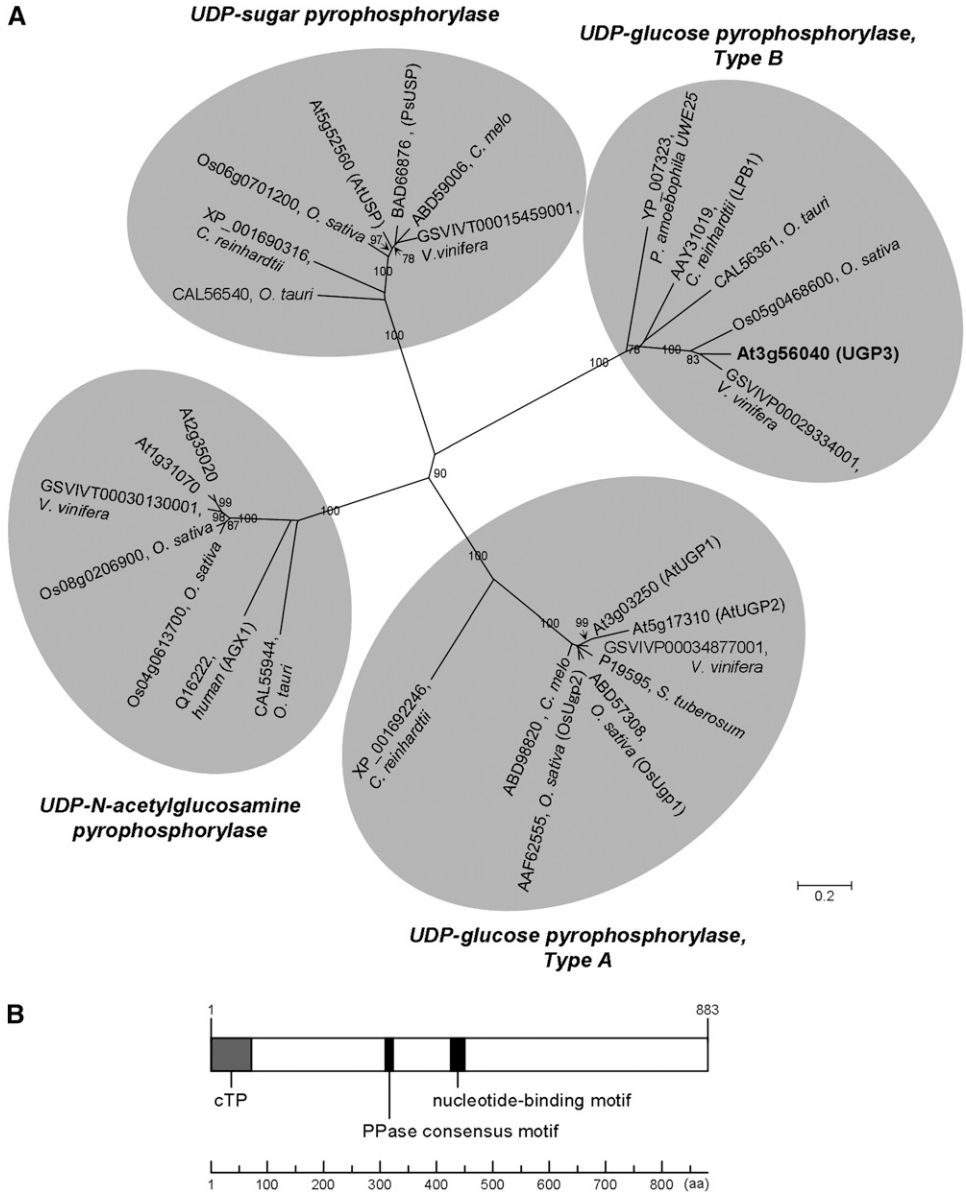

Figure 4. Unrooted Phylogenetic Tree of UDP-Hexose Pyrophosphorylases.

(A) Unrooted phylogenetic tree of UDP-hexose pyrophosphorylases. A total of 28 amino acid sequences were aligned using the ClustalX program, and the tree was constructed based on the neighbor-joining method using MEGA4 software. The bar indicates substitutions per site. Bootstrap values (1000 replicates) above 70% are shown on branches. The names of the proteins are shown in parentheses when they have already been reported.
(B) Schematic representation of the structure of the UGP3 protein. Regions of possible cTPs, pyrophosphorylase (PPase) consensus motif, and nucleotide binding motif are shown in black boxes.

detected. Contamination of the chloroplastic fraction by proteins from the cytosol was checked by measuring the activity of cytosolic marker protein, alcohol dehydrogenase (ADH), because plants are supposed to have substantial UGPase activity in the cytosol (Kleczkowski et al., 2004). On the basis of the ADH activities in the enzyme extracts from whole leaves and chloroplastic fractions, the respective amounts of UGPase activity attributable to cytosolic proteins were estimated to be 7, 14, and 13% of the UGPase activities in the chloroplastic fractions from the wild type, *ugp3-1*, and *ugp3-2*, indicating that protein contamination from the cytosol could not explain the decrease of UGPase activity in the chloroplast fraction of *ugp3* mutants. UGPase activities in whole leaves of the wild type, *ugp3-1*, and *ugp3-2* were determined to be 56.5 $\pm$ 4.6, 48.1 $\pm$ 7.3, and 51.5 $\pm$ 5.7 (pkatal g^{-1} fresh weight), respectively. Levels of UDP-Glc in whole leaves of the wild type, *ugp3-1*, and *ugp3-2* were

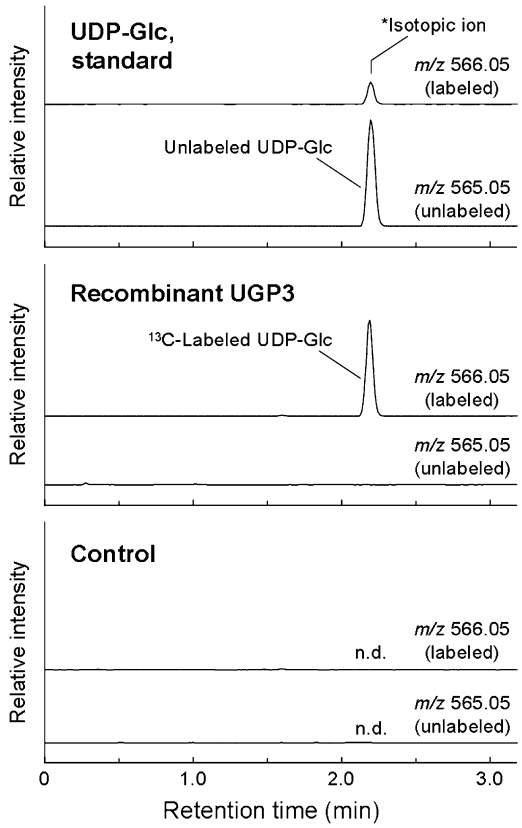

Figure 5. Analysis of the Reaction Product of Recombinant UGP3.

The UGP3 recombinant protein was incubated with [1-^{13}C]Glc1P and UTP, and reaction products were analyzed using UPLC-Q-MS. The protein fraction from *E. coli* carrying a control vector was used as a control. Unlabeled and labeled UDP-Glc were monitored by selected ion monitoring of their $[M–H]^-$ ions at *m/z* 565.05 and 566.05, respectively. The intensity of the peak of $[M–H]^-$ of standard UDP-Glc (50 pmol) observed at *m/z* 565.05 was set as 100%. The baseline was shifted for convenience in each panel. The asterisk indicates the peak attributable to the isotopic ions (M+1) containing single naturally existing ^{13}C, ^{2}H, or ^{15}N. n.d., not detected.

determined to be 57.8 ± 3.8, 63.6 ± 5.4, and 59.3 ± 4.3 (μg g^{-1} fresh weight), respectively. These results indicate that the total levels of UGPase activity and UDP-Glc in leaves are only slightly affected by knockout of the *UGP3* gene.

The Effects of Phosphate and Sulfate Starvation on Lipid Composition

Phosphate deprivation is known to induce an increase in levels of SQDG in the leaves of *Arabidopsis* to compensate for the decrease in phospholipids, especially PG, through activation of expression of *SQD1* and *SQD2* (Essigmann et al., 1998; Yu et al., 2002). Based on the results of gene expression analysis shown in Supplemental Figure 2 online, it was expected that the expression of the *UGP3* gene would be elevated by phosphate limitation along with *SQD1* and *SQD2*. As expected, quantitative PCR revealed that the expression of the *UGP3* gene was increased almost 15-fold by phosphate limitation compared with that under phosphate-sufficient growth conditions (see Supplemental Figure 13 online). To investigate the effects of lack of SQDG on lipid metabolism in the *ugp3* mutants under phosphate-limiting conditions, polar glycerolipid composition was compared in extracts from leaves of wild-type plants and *ugp3* mutants grown in the presence and absence of phosphate. In addition, another SQDG-deficient mutant of *Arabidopsis*, *sqd1*, was also subjected to the phosphate starvation experiment to reveal the physiological function of *UGP3* in lipid metabolism in detail. The mutants *ugp3* and *sqd1*, deficient in SQDG, accumulated slightly more PG compared with the wild type under phosphate-sufficient growth conditions (Figure 7A). Under phosphate-limiting conditions, the relative amount of SQDG increased by approximately fourfold, and PG amounts decreased by half in the wild type, while SQDG was not detected and PG only slightly decreased in *ugp3* and *sqd1* mutants. Phosphorus limitation also caused a decrease in other phospholipids (PE and PC) and an increase in DGDG in the wild type, *ugp3*, and *sqd1*, but the amounts of decrease and increase in these lipid classes were similar among the wild type, *ugp3*, and *sqd1*.

Because SQDG contains sulfur in the polar headgroup, the effect of sulfur limitation on the profiles of polar glycerolipids was also examined. The expression level of *UGP3* in leaves of wild-type plants grown under sulfate-depleted conditions for 2 d was about half of that under sulfate-sufficient growth conditions (see Supplemental Figure 13 online). However, sulfur limitation did not necessarily lead to a significant decrease in the relative level of SQDG in the wild type (Figure 7B). In addition, the contents of other polar glycerolipids in the wild type were not as significantly affected by this short-duration sulfur limitation.

UGP3 Homologs Are Evolutionally Conserved across Plant Species

UGP3 homologs are found in several plant species (Figure 4A), suggesting that these proteins are evolutionally conserved across plant species. To determine the evolutionary relationship among *UGP3* homologs, a comparative genomics study was

Table 1. Substrate Specificity of Recombinant UGP3 toward Monosaccharide Monophosphates

Monosaccharide Monophosphate	Relative Activity (%)
Glucose-1-phosphate	100
Galactose-1-phosphate	14.2 ± 3.8
N-Acetylglucosamine-1-phosphate	n.d.
Glucosamine-1-phosphate	n.d.
Mannose-1-phosphate	n.d.
Fucose-1-phosphate	n.d.
Glucose-6-phosphate	n.d.
Mannose-6-phosphate	n.d.

Activities of recombinant UGP3 for various alternative monosaccharide monophosphates (0.5 mM) were assayed in the presence of UTP (0.5 mM) and expressed as a percentage of that for Glc1P. n.d., not detected.

Table 2. Effect of Magnesium Ion on UGPase Activity of UGP3

Mg^{2+} (mM)	Relative Activity (%)
30.0	100
10.0	98 ± 7.4
5.0	90 ± 5.7
1.0	51 ± 7.8
0.5	38 ± 11
0.1	3.8 ± 2.8
0.0	n.d.

Activities of recombinant UGP3 were assayed in the presence of UTP (0.5 mM), [1-^{13}C]Glc1P (0.5 mM), and various amounts of $MgCl_2$. Relative activities are expressed as a percentage of that obtained in the presence of 30 mM $MgCl_2$. n.d., not detected.

performed on *UGP3* homologs in four higher plant species (*Arabidopsis*, *Populus trichocarpa*, *V. vinifera*, and *O. sativa*) for which whole-genome sequences are available. All of these species possess *UGP3* homologs as a single-copy gene (Figure 8A). The *UGP3* homologs found in these species are highly divided by introns (Figure 8A), but the number and size distribution of exons within the coding sequences are highly conserved in these species (Figure 8B) and the genome region coding two important motifs for UGPase activity, pyrophosphorylase consensus and nucleotide binding motifs, are found in the corresponding exons. In addition, all of the *UGP3* homologs from these four plant species have been shown to have a putative region coding chloroplastic transit peptides at the first exons, as determined by TargetP. The syntenic relationships among the *UGP3* homologs across the four plant species were also analyzed using the Plant Gene Duplication Database (PGDD; http://chibba.agtec.uga.edu/duplication/), which revealed cross-genome syntenic relationships among Ath:At3g56040, Ptr:gw1.X.1665.1, and Vvi:GSVIVP00029334001 (Figure 8A; see Supplemental Figure 14 online). These studies suggest a close evolutional relationship and a shared function of the *UGP3* homologs in higher plants.

The orthologs of *UGP3* homologs also can be found in the genomes of lower plants, *Selaginella moellendorffii* and *C. reinhardtii*. In addition, the genomic region and EST homologous to the sequence of *UGP3* homologs in higher plants can be found in *Physcomitrella patens*, although the corresponding full-length sequences of transcripts and amino acids are not available (see Supplemental Figure 15 online). The exon-intron structures of the genes in *S. moellendorffii* and *C. reinhardtii* were analyzed and compared with those of higher plants (see Supplemental Figure 16 online). The putative homolog in *S. moellendorffii* has 18 exons divided by relatively short introns (see Supplemental Figure 16A online), but the number and size distribution of exons within the coding sequences are very similar with those of higher plants (see Supplemental Figure 16B online). The putative homolog in *C. reinhardtii* (*LPB1*) has a much smaller number of exons that are differently organized compared with other plants (see Supplemental Figure 16 online). These indicated that the higher plants inherited the basic genomic structure of type B UGPases from ferns, and the structures of introns have diverged through the evolution of higher plants.

DISCUSSION

Transcriptome Coexpression Analysis Efficiently Extracts Coordinately Expressed Genes Involved in Glycoglycerolipid Biosynthesis

SQDG serves to maintain the proper balance of anionic charge in the thylakoid membrane, especially under phosphate-limiting conditions, and thus is considered to be of conditional importance in plants. In this study, an unknown gene involved in SQDG biosynthesis was efficiently targeted using transcriptome coexpression analysis, and its function was determined using a combination of reverse genetics, reverse biochemistry, and detailed lipid profiling. Transcriptome coexpression analysis also showed that *MGD2* and *MGD3*, not involved in SQDG biosynthesis, were grouped into the same cluster with SQDG biosynthetic genes (Figure 2). *MGD1*, *MGD2*, and *MGD3* encode 1,2-diacylglycerol 3-β-galactosyltransferases, the final enzymes for MGDG synthesis. Among these genes, only *MGD1* is highly expressed in all tissues of *Arabidopsis*, whereas expression of *MGD2* and *MGD3* are observed only in restricted parts, such as leaf tips and pollen grains (Kobayashi et al., 2004). These tissue-specific expression patterns of *MGD2/3* are not that similar to those of *SQD1*, *SQD2*, and *UGP3*. However, a previous study also reported that *MGD2/3*, but not *MGD1*, were strongly induced during phosphate starvation in *Arabidopsis* (Awai et al., 2001; Kobayashi et al., 2004) and that these upregulations of *MGD2/3* are known to be regulated by auxin/cytokinin crosstalk (Kobayashi et al., 2006). As shown in Figure 2, the correlation coefficients between genes involved in sulfolipid and galactolipid biosynthesis were increased in the hormone treatment data set compared with all data sets. These results suggest a shared hormonal regulation system for SQDG biosynthetic genes and *MGD2/3*, although it remains unclear whether the shared regulation system can be fully explained by the auxin/cytokinin crosstalk model.

Two other genes, At2g42690 and At1g08310, are also grouped in the same cluster with *UGP3*. The functions of these genes have not been determined, but they may also be involved in glycoglycerolipid metabolism under phosphate-limiting conditions, since these genes are annotated as lipase and esterase/lipase/thioesterase family proteins, respectively.

Table 3. Effect of Pyrophosphate on UGPase Activity of UGP3

Pyrophosphate (mM)	Relative Activity (%)
0.00	100
0.25	57 ± 8.4
0.50	19 ± 5.4
1.00	11 ± 6.2
5.00	3.2 ± 2.2
10.00	1.5 ± 1.2

Activities of recombinant UGP3 were assayed in the presence of UTP (0.5 mM), [1-^{13}C]Glc1P (0.5 mM), and various amounts of sodium pyrophosphate. Relative activities are expressed as percentages of that obtained without addition of pyrophosphate.

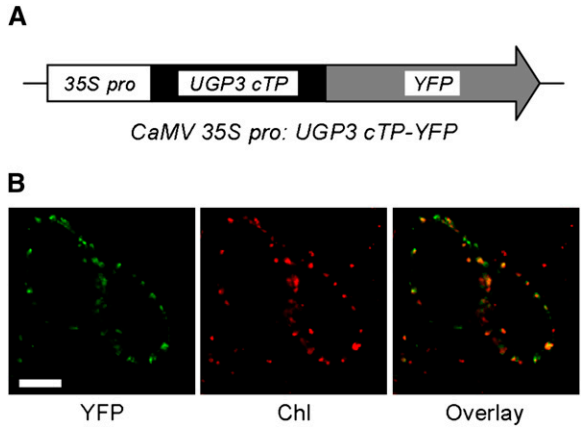

Figure 6. Confocal Micrographs Showing Chloroplast Targeting of UGP3.

(A) Schematic drawing of the construct encoding predicted chloroplastic transit peptides of UGP3 and YFP used to transform cultured *Arabidopsis* cells. The transgene consists of a fragment encoding N-terminal 200 peptides including putative cTPs (72 peptides) of UGP3 under the control of the constitutive cauliflower mosaic virus 35S promoter.

(B) Subcellular localization of UGP3. The first column shows the green fluorescence image derived from YFP, the second shows red autofluorescence from chlorophylls, and the third shows an overlay of the two channels. Bar = 20 μm.

UDP-Glc for SQDG Synthesis Is Generated inside Chloroplasts by UGP3

UDP-galactose, a precursor of galactolipids synthesized in chloroplasts, is widely assumed to be incorporated from the cytosol (Benning and Ohta, 2005) because the concentration of UDP-galactose is very low inside plastids and high in the cytosol (Bligny et al., 1990) and because MGDG synthase, MGD1, is located on the outside of the inner chloroplastic envelope membrane (Xu et al., 2005). UDP-Glc for SQDG biosynthesis has also been speculated to be of cytosolic origin, and certain proteins have been proposed as the candidate transporters of UDP-Glc for SQDG biosynthesis (Knappe et al., 2003). However, a feeding experiment in which radiolabeled UDP-Glc was applied to isolated chloroplasts of the pea revealed that radioactivity was not efficiently incorporated into the sulfoquinovose moiety (Roy and Harwood, 1999), raising the question of how UDP-Glc is transported to the chloroplasts. This study revealed that UDP-Glc for SQDG biosynthesis is generated in the chloroplasts by the UGP3 protein, not incorporated from extrachloroplastic space (Figure 9). Two substrates for UGP3 are found in the chloroplasts (Glc1P can be supplied by the pathway for starch biosynthesis, and UTP is the substrate for RNA synthesis). In *Arabidopsis*, phosphate limitation leads to upregulation of one of other UGP genes, *UGP1*, and a corresponding increase in UGPase activity (Ciereszko et al., 2001), suggesting the possibility that UDP-Glc for SQDG biosynthesis is partially supplied by inducing activity of the UGP1 protein under phosphate-limiting conditions. However, *ugp3* mutants grown under phosphate-limiting conditions accumulate no SQDG (Figure 7A), indicating that there are no alternative pathways for supplying UDP-Glc for SQD1, even under conditions that induce enhanced accumulation of SQDG.

Although UDP-Glc is generally considered to be synthesized exclusively in the cytosol, UGPase activity has been reported in chloroplasts in the leaves of tobacco (*Nicotiana tabacum*) (Bird et al., 1965), rice, and bean (*Phaseolus vulgaris*) (Nomura et al., 1967). Measurements of UGPase activity in intact chloroplasts isolated from the rosette leaves of *Arabidopsis* revealed that UGPase activity in the *ugp3* mutants was about half of that in the wild type (see Supplemental Figure 13 online). This is a reasonable result if the native UGP3 protein does have UGPase activity in the chloroplasts, but poses a question regarding the origin of the residual UGPase activity in the knockout lines. Analysis of the activity of the cytosolic marker protein showed that contamination by cytosolic UGPase activity could not fully explain the residual UGPase activity in *ugp3*. In *Arabidopsis*, there are six genes annotated as UDP-hexose pyrophosphorylases (Figure 4A). Subcellular localizations of the products of these genes have not been directly confirmed by experimental evidence, except for UGP3. Thus, there is a possibility that another UGPase is localized in the chloroplasts, as is UGP3. In this case, UDP-Glc generated by UGP3 should be specifically supplied for SQD1, presumably through a substrate channeling mechanism or suborganelle compartmentation. There is also the possibility that certain cytosolic UDP-hexose pyrophosphorylases might be bound to the surface of the chloroplasts but are not found inside the chloroplasts. To understand the origin of the residual UGPase activity in isolated chloroplastic fractions of *ugp3*, further studies of other possible UDP-hexose pyrophosphorylases would be required.

Knockout of the *UGP3* Gene Causes Compositional Changes of Anionic Lipids in Chloroplasts and Conditionally Affects the Biosynthesis of Galactolipid

Slight increases in the amount of PG were observed in *ugp3* mutants compared with the wild type under normal growth conditions (Figures 3 and 7). Under phosphate-limiting conditions, the relative amount of SQDG increased and the amount of PG decreased in the wild type, whereas SQDG was not detected and PG barely decreased in the *ugp3* and *sqd1* mutants (Figure 7). These results are consistent with previous reports on the *sqd2* mutant and support the theory that the amounts of SQDG and PG are reciprocally controlled in plants to maintain the proper balance of anionic charge in the thylakoid membrane (Benning et al., 1993; Güler et al., 1996; Yu et al., 2002, 2003).

In addition to these changes in lipid accumulation patterns in *ugp3* mutants, also observed in *sqd2* (Yu et al., 2002), the relative amount of MGDG seemed to slightly decrease in the *ugp3* mutant compared with the wild type under phosphate-sufficient growth conditions (Figure 7). Although the *sqd1* mutant lacked SQDG, as did *ugp3*, the relative amount of MGDG in *sqd1* was similar to that of the wild type under phosphate-sufficient and phosphate-limiting conditions. These results suggest that knockout of the *UGP3* gene has a slight effect on MGDG biosynthesis in a condition-dependent manner.

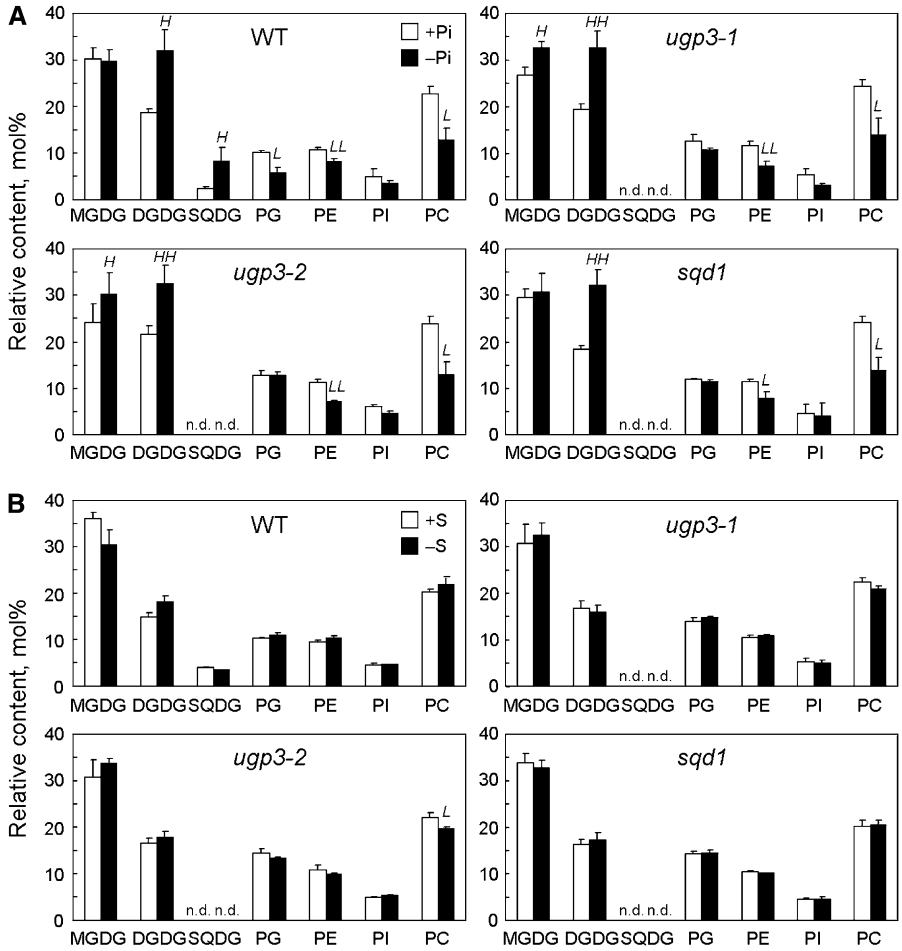

Figure 7. Analyses of Polar Glycerolipids in the Wild Type and *ugp3* Mutants under Phosphate- and Sulfate-Limiting Conditions.

Crude lipid extracts from leaves of *Arabidopsis* grown under phosphate- and sulfate-controlled conditions were separated using thin layer chromatography, followed by derivatization and analysis by gas chromatography. The amount of each lipid class was calculated based on the amount of fatty acid methylesters. The amount of each lipid class was expressed relative to the sum of the amounts of the polar glycerolipid classes. Each data point expresses the mean of three experiments ± SD. $^{H, HH}$ The value for the plant grown under nutrition-depleted conditions is higher than the value under nutrition-sufficient conditions ($^{H}P < 0.05$, $^{HH}P < 0.01$, Student's *t* test). $^{L, LL}$ The value for the plant grown under nutrition-depleted conditions is lower than the value under nutrition-sufficient conditions ($^{L}P < 0.05$, $^{LL}P < 0.01$, Student's *t* test). n.d., not detected.

(A) Composition of polar glycerolipids in wild-type, *ugp3-1*, *ugp3-2*, and *sqd1* plants under phosphate-sufficient (+P, 10 mM) or phosphate-depleted (–P, 0 mM) conditions.

(B) Composition of polar glycerolipids in wild-type, *ugp3-1*, *ugp3-2*, and *sqd1* plants under sulfate-sufficient (+S, 1.5 mM) or sulfate-depleted (–S, 0 mM) conditions.

UDP-Glc is an important metabolite used for synthesis of various kinds of glycosides and saccharides. To reveal the function of *UGP3* in more detail, methanolic extracts of rosette leaves were subjected to untargeted reversed-phase LC-MS analysis. Methanolic extracts of *Arabidopsis* leaves contain glycosides, such as flavonoids and glucosinolates, and compounds synthesized from glycosylated precursors, such as sinapoylmalate. The amounts of these compounds were nearly the same between the wild type and *ugp3* mutants, and no significant changes in the amounts of specific metabolites could be found between the wild type and *ugp3* mutants (see Supplemental Figure 7 online). These data suggest that UDP-Glc for biosynthesis of secondary metabolites and cellulose can be sufficiently supplied by other UGPases, such as UGP1 and UGP2, which are thought to be localized in the cytosol in *Arabidopsis* (Meng et al., 2008).

UGP3 and Its Homologs Are Unique UGPases Found in Plants

Phylogenic analysis revealed that UGP3 belongs to a novel protein family, type B UGPases, with biochemically uncharacterized proteins from the higher plants (*V. vinifera*, *P. trichocarpa*, and *O. sativa*) and two unicellular green algae (*O. tauri* and *C.*

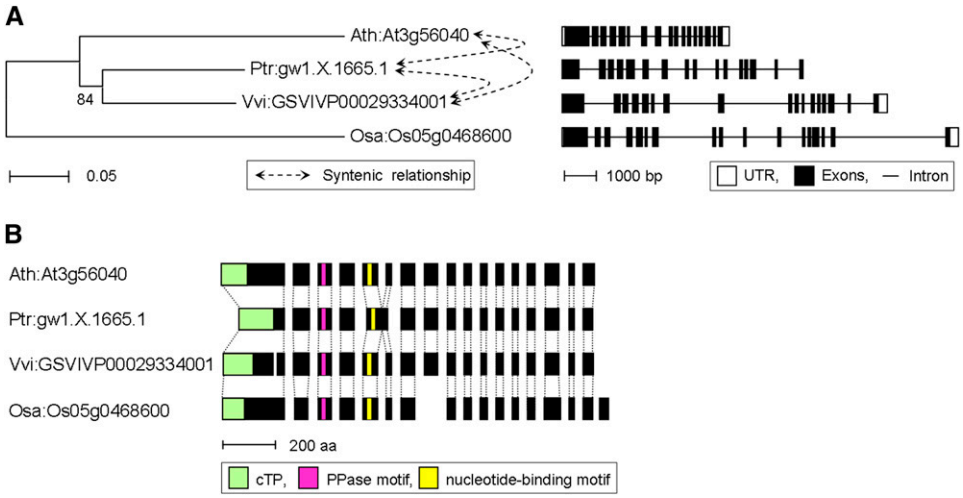

Figure 8. Evolutional Studies of the *UGP3* Homologs in Higher Plants.

(A) Left: Phylogenetic relationships of the UGP3 proteins in higher plants. The unrooted phylogenetic tree was constructed by alignment of deduced amino acid sequences from *Arabidopsis* (Ath), *P. trichocarpa* (Ptr), *V. vinifera* (Vvi), and *O. sativa* (Osa). The bar indicates substitutions per site. Bootstrap values (1000 replicates) are shown on branches. Dashed arrows indicate gene pairs in terms of cross-genome syntenic relationships. Right: Exon-intron structures of the *UGP3* genes. The untranslated region (UTR) sequences are shown when available. Open boxes represent UTRs; solid boxes, coding regions; and solid lines, introns.
(B) The number and size distribution of exons within the coding sequences of *UGP3* homologs.

reinhardtii) as close homologs (Figures 4 and 8), which likely exhibit substrate specificity similar to that of UGP3 in *Arabidopsis*. UGP3 exhibited a high specificity for Glc1P, followed by Gal1P as glycosyl donor (Table 1). At the amino acid level, the most closely related proteins to type B UGPases are USPases, which catalyze the conversion of various monosaccharide-1-phosphates to their respective UDP-sugars (Figure 4) (Kotake et al., 2004, 2007; Litterer et al., 2006). The property that UGP3 accepts Gal1P as a poor substrate may be related to the sequence similarity with USPases.

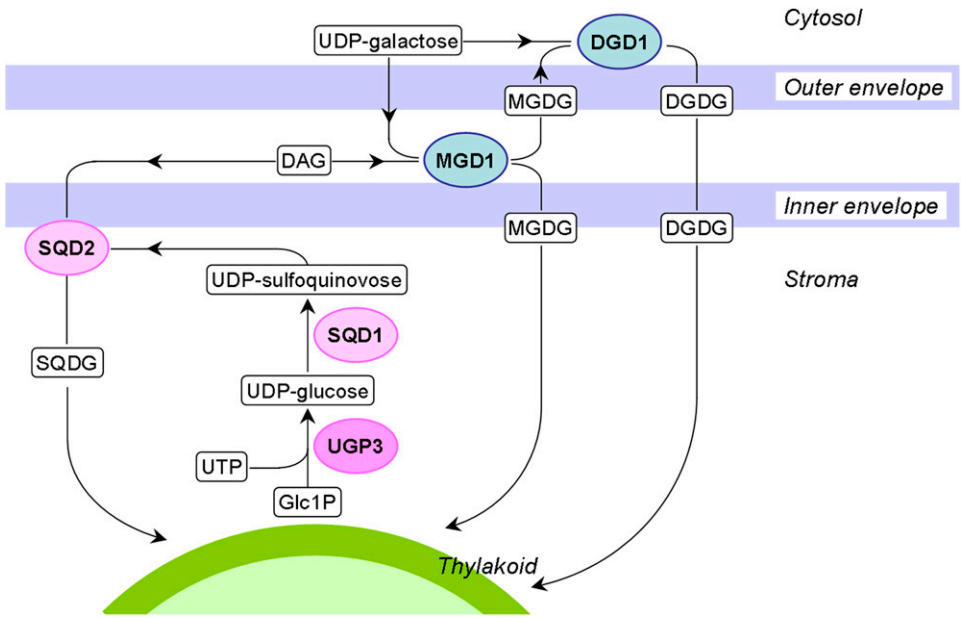

Figure 9. Proposed Biosynthetic Pathway for Sulfolipid and Galactolipids in Chloroplasts.

Biosynthetic schemes for three glycoglycerolipids under normal growth conditions are illustrated along with the pathway involving UGP3.

Comparative genomics analysis of *UGP3* homologs revealed the conservation of gene structures and cross-genomic syntenic relationships in several model plants, suggesting a close evolutional relationship and a shared function of *UGP3* homologs in higher plants (Figure 8; see Supplemental Figure 16 online). *Arabidopsis* has another type of UGPase family proteins, UGP1 and UGP2, which can catalyze the formation of UDP-Glc as can UGP3. To investigate the distributions of these UGPases, homologs of type A UGPases were investigated in four plant species (*Arabidopsis*, *P. trichocarpa*, *V. vinifera*, and *O. sativa*) as *UGP3* homologs. All of these four plant species have one or two genes coding type A UGPase homologs (see Supplemental Figure 17 online). These results suggest that plants possess two different types of UGPases, and the presence of each subfamily, conserved throughout plant evolution, could be profitable for metabolism of UDP-sugars in plants.

LPB1 of *C. reinhardtii* is one of the close homologs of UGP3, and the only one of these proteins whose function has been investigated (Chang et al., 2005). The *lpb1* mutant was reported to die more rapidly than the wild type during phosphorus and sulfate limitation. If LPB1 has the same physiological function as UGP3 in *C. reinhardtii*, the amount of SQDG in *lpb1* might be decreased compared with the wild type. There are common visible phenotypes observed in *lpb1* and a SQDG-deficient mutant of *C. reinhardtii*, Δ*sqd1* (Riekhof et al., 2003). The growth of both mutants ceases faster than the wild type under phosphate-depleted conditions. In addition, both mutants are more sensitive to 3-(3,4-dichlorophenyl)-1,1-dimethylurea (DCMU), a herbicide binding to the Q_B acceptor site of photosystem II, than the wild type, suggesting changes in the chemistry of photosystem II. Another SQDG-deficient mutant of *C. reinhardtii*, *hf-2*, also shows enhanced sensitivity to DCMU compared with the wild type, although the exact molecular defect is not known (Sato et al., 1995; Minoda et al., 2002). Since *C. reinhardtii* is apparently a distinct organism from *Arabidopsis*, LPB1 may also have quite different physiological functions from UGP3. In contrast with *lpb1*, *ugp3* mutants of *Arabidopsis* did not show as severe growth defects compared with the wild type when they were grown under phosphate- and sulfate-limiting conditions. As described by Chang et al. (2005), LPB1 may play a role in some aspect of polysaccharide metabolism and/or influence phosphorus metabolism (either structural or regulatory) in a way that is critical for allowing the cells to acclimate to nutrient-deficient conditions.

Orthologs of Three SQDG Biosynthetic Genes Are Differently Distributed among Organisms

Orthologs of *SQD1* and *SQD2* of *Arabidopsis* can be found in cyanobacteria, which are thought to be closely related to the ancestral bacteria of chloroplasts (Essigmann et al., 1998; Yu et al., 2002). Therefore, it was expected that orthologs of *UGP3* in *Arabidopsis* could also be found in cyanobacteria. However, a counterpart for *UGP3* was not found in cyanobacteria. Thus, UDP-Glc for SQDG is synthesized or supplied for UDP-SQ synthase by a different mechanism in cyanobacteria. In comparison to the case of cyanobacteria, a homologous protein sequence was found in *Candidatus Protochlamydia amoebophila* UWE25. UWE25 is an endosymbiotic chlamydial species that is thought to have diverged from the Chlamydiaceae ~700 million years ago. A number of putative plant genes with significant similarity to UWE25 have been localized to the chloroplast, suggesting their involvement in the development of endosymbiosis of a cyanobacterium in Plantae ancestry (Horn et al., 2004; Moustafa et al., 2008). In contrast with *UGP3*, sequences homologous to *SQD1* and *SQD2* are not found in UWE25. These results suggest that the SQDG biosynthetic pathway in plants is not simply inherited from cyanobacteria. Most likely, a symbiotic chlamydia-like cell provided an ancient *UGP3* gene to a Plantae ancestor by horizontal gene transfer, and the host cell gradually developed a new regulated metabolic connection between the newly established endosymbiont (cyanobacterium) and the host cell.

UGP3 and Two Other SQDG Biosynthetic Genes Are Differentially Regulated in *Arabidopsis* Starved for Sulfate

In addition to being a constituent of the lipid bilayer of thylakoid, SQDG is presumed to play a sulfur storage role as one of the major sulfur-containing organic compounds in higher plants. Sulfite generated via the sulfur assimilation pathway is directly incorporated into UDP-SQ (Leustek and Saito, 1999; Saito, 2004). In this study, the amount of SQDG in leaves did not markedly decrease when the plants were grown under sulfur-limiting conditions for 2 d. However, sulfur limitation for a longer time has been reported to lead to a decrease in SQDG in the leaves of *Arabidopsis* to conserve the sulfur in plants (Nikiforova et al., 2005). To understand the regulation of the genes involved in the SQDG biosynthetic pathway under sulfur-limiting conditions, changes in the expression levels of *SQD1*, *SQD2*, and *UGP3* in response to sulfur deprivation were analyzed based on transcriptome data provided by the AtGenExpress Visualization Tool (Schmid et al., 2005). As observed in this study, sulfur limitation induced a decrease in the expression of *UGP3* compared with sulfur-sufficient conditions, while the expression of *SQD1* and *SQD2* was hardly affected, at least during the first 24 h after transfer of the *Arabidopsis* plants to a sulfur-depleted medium (see Supplemental Figure 18 online). These data suggest that the expression of *UGP3* is more strictly controlled than the other two SQDG biosynthetic genes when *Arabidopsis* is transferred to a sulfur-depleted medium, perhaps to reduce the supply of UDP-Glc for SQDG biosynthesis. Downregulation of the gene involved in the farthest upstream reaction step specific to SQDG biosynthesis is reasonable in terms of saving sulfur and carbohydrates.

As described above, *UGP3* and the other two SQDG biosynthetic genes in *Arabidopsis* are likely to be differentially regulated under sulfate-limiting conditions. Recently, a transcription factor, *SLIM1*, which is a central transcriptional regulator of plant sulfur response and metabolism, was isolated from *Arabidopsis* (Maruyama-Nakashita et al., 2006). A series of –S-responsive SLIM1-dependent genes were reported, and one of them was found to be *UGP3*, but not *SQD1* or *SQD2*. Under sulfur-limiting conditions, expression of *UGP3* decreases in the wild type, while a decrease in the expression of *UGP3* is suppressed in *slim1* mutants. These results suggest that the expression of *UGP3* and

the other two SQDG biosynthetic genes are coordinately regulated under normal and phosphate-limiting conditions, but they are differently regulated when they are starved for sulfate. These differences in transcriptional regulation may be derived from a difference in their evolutional origins.

METHODS

Chemicals

α-D-[1-^{13}C]glucopyranose-1-phosphate (99 atom-% ^{13}C) and α-D-galactopyranose-1-phosphate were purchased from Omicron Biochemicals and Calbiochem, respectively. UDP-Glc, UTP, and solvents for LC-MS were obtained from Wako Pure Chemical Industries. Other UDP-hexoses, nucleotide triphosphates, and sugar monophosphates were purchased from Sigma-Aldrich. SQDG and glucoside of sitosterol were obtained from Larodan Fine Chemicals. Hydrogenated MGDG and hydrogenated DGDG were purchased from Matreya. Phospholipid standards (PC, PE, PG, PA, and PI) and glucosyceramide from soybeans were obtained from Avanti Polar Lipids.

Plant Materials

Seeds of the T-DNA insertion line for the *ugp3-1*, *ugp3-2*, and *sqd1* mutants (SALK_020654, SALK_073806, and SALK_016799, respectively) were obtained from the ABRC. The T-DNA insertion site was confirmed by sequencing of PCR fragments. The primers used for this study are listed in Supplemental Table 1 online. The PCR fragment at the left border of the T-DNA was amplified using *LBa1* and gene-specific primers (*ugp3-1_Rv* for SALK_020654, *ugp3-2_Rv* for SALK_073806, and *sqd1_Rv* for SALK_016799). Unless stated otherwise, plants were grown on agar-solidified Murashige and Skoog (MS) medium containing 1% (w/v) sucrose at 22°C under a 16-h-light/8-h-dark cycle. After an 18-d incubation, the aerial regions were harvested 6 h after the onset of the light phase. For lipid analyses of plants grown under phosphate-controlled conditions, wild type (Columbia-0 accession) plants, *ugp3-1*, *ugp3-2*, and *sqd1* mutants were grown on phosphate-controlled medium with sufficient phosphate (10 mM) for 10 d and then transferred to either phosphate-sufficient (10 mM) or phosphate-depleted (0 mM) medium prepared as described by Härtel et al. (2000) and grown for another 10 d. For lipid analyses of plants grown under sulfate-controlled conditions, plants were grown on MS medium for 10 d and then transferred to either MS medium or sulfate-depleted (0 mM) MS medium by replacing $MgSO_4$ with $MgCl_2$ for another 2 d. For isolation of intact chloroplasts, plants were grown on soil at 22°C under a 16-h-light/8-h-dark cycle for 45 d.

Coexpression Analyses

Coexpression analyses were performed using a Coexpression Gene Search algorithm on the RIKEN PRIMe website (Akiyama et al., 2008) based on ATTED-II (Obayashi et al., 2007). The Coexpression Gene Search program is a web-based application designed to identify correlated genes from gene expression data produced using transcriptome data. All data sets of version 3 of ATTED II (tissue and development, stress treatments, and hormone treatments) were used for the analyses as described by Yonekura-Sakakibara et al. (2007). At first, the coexpression relationship among all genes described below was analyzed by the Coexpression Gene Search program (matrix, all data sets v.3; method, interconnection of sets; threshold value, +0.5), and highly coexpression gene clusters were narrowed down. Then, these coexpressing genes were newly utilized for query for Coexpression Gene Search (matrix, all data sets v.3; method, intersection of sets; threshold value, +0.5). Genes that coexpressed with at least two of the query genes were selected, with considering annotations for gene functions. Then, the expression coefficient of these selected genes was analyzed again by Coexpression Gene Search program, and the result was downloaded as a Pajek file. Then, coexpressing gene pairs were visualized by connecting with lines using a network analysis program, Pajek (http://vlado.fmf.uni-lj.si/pub/networks/pajek/). We applied a layout algorithm (Kamada-Kawai) by selecting from the layout menu in the Pajek software to adjust the layout of the nodes. Finally, the layout was adjusted manually. The genes used for queries in the transcriptome coexpression analysis were as follows: At4g31780 (*MGD1*), At5g20410 (*MGD2*), At2g11810 (*MGD3*), At3g11670 (*DGD1*), At4g00550 (*DGD2*), At4g33030 (*SQD1*), At5g01220 (*SQD2*), At2g01180 (*PAP1*), At1g15080 (*PAP2*), At1g62430 (*CDS1*), and At2g39290 (*PGS1*).

LC-MS Analysis of Lipid Extracts

Total lipids were extracted according to the method of Bligh and Dyer (1959). Crude lipid extracts were dissolved in chloroform and subjected to LC-MS analysis using a Shimadzu LCMS-IT-TOF mass spectrometer combined with a Shimadzu LC-20AD HPLC system. A two-solvent system was used to generate the mobile phase: solvent A, methanol-water (95:5, v/v) containing 0.2% ammonium formate, pH 5.9; solvent B, acetonitrile-methanol-water (95:2:3, v/v/v) containing 0.2% ammonium formate, pH 5.9. The pH of both solvents A and B was adjusted by adding 30% NH_4OH to the mixtures of solvents containing 0.2% (v/v) formic acid. At the beginning of the gradient, the mobile phase was 100% solvent B for 3.33 min. Solvent B was linearly decreased to 60% over 6.67 min and successively decreased to 30% over 1.33 min. Solvent B was held at 30% for 3.33 min and then increased to 100% for reequilibration. The flow rate was held 0.18 mL min^{-1} for 3.33 min at the beginning of the gradient and linearly increased to 0.2 mL min^{-1} over 11.33 min. The flow rate was then increased to 0.4 mL min^{-1} at 14.66 min after the beginning of the gradient, maintained for 13.33 min, and then decreased to 0.18 mL min^{-1}. Total elution time was 40 min.

High-resolution ESI-MS were acquired in both positive and negative ion modes by switching the polarity during individual analyses. Conditions for measurement of ESI-MS were as follows: mass range, *m/z* 150 to 1600; interface voltage, 4.5 V; curved desolvation line temperature, 200°C; heat block temperature, 200°C; ion accumulation time, 10 ms; detector voltage, 1.80 kV; nebulizer gas, N_2 (15 L·min^{-1}). The collision-induced dissociation experiment was performed using Ar as the collision gas, with a relative collision energy of 50% and a relative collision gas flow of 50%.

Peak areas of individual lipid molecules were calculated based on the *m/z* values of their molecular-related ions or fragment ions. The ions used for calculation of peak areas are as follows: $[M+HCOO]^-$ for MGDG and DGDG, $[M-H]^-$ for SQDG and PI, $[M+NH_4-\text{phosphoglycerol}]^+$ for PG, $[M+NH_4-\text{phosphoethanolamine}]^+$ for PE, and $[M+H]^+$ for PC. Because the lipid species with the same polar head were eluted at almost the same retention time (see Supplemental Figure 5 online), corrections for overlap of isotopic variants in higher mass lipids were applied.

Ionization efficiency is largely influenced by the nature of the polar headgroups. Thus, the ionization efficiency is assumed to be almost identical when molecules have the same polar headgroups. Levels of individual lipid molecules in the wild-type plant and mutant lines were expressed as relative values against the sum of the peak areas of lipid molecules with the same polar headgroups in the wild type (Figure 3).

Lipid and Fatty Acid Analyses Using Thin Layer Chromatography and Gas Chromatography–Mass Spectrometry

Lipids from plants grown under phosphate- and sulfate-depleted conditions were extracted and analyzed using thin layer chromatography and gas chromatography–mass spectrometry. The lipids were separated

using two-dimensional thin layer chromatography followed by fatty acid detection and measurement of membrane lipid content as described by Kobayashi et al. (2007).

Quantitative Real-Time RT-PCR

Total RNA was isolated using the SV Total RNA Isolation System (Promega) according to the manufacturer's instructions. Reverse transcription was performed using the PrimeScript RT Reagent Kit (Takara Bio). cDNA amplification was performed using the SYBR *PreMix Ex Taq* (Takara Bio) and 400 nM gene-specific primers. Real-time PCR was performed using the SYBR Green Perfect Real Time Kit (Takara Bio) and the Thermal Cycler Dice Real Time System. mRNA contents were calculated using eIF4A as an internal standard. Three biological replicates were used for quantitative real-time PCR. Gene-specific primers are described in Supplemental Table 1 online.

Phylogenetic Analysis

Protein sequences were obtained using homologous protein cluster data consisting of protein sequences of *Arabidopsis thaliana* (The Arabidopsis Information Resource [TAIR]; ftp://ftp.Arabidopsis.org/home/tair/Sequences/), *Oryza sativa* (The Rice Annotation Project Database [RAP-DB]; http://rapdb.dna.affrc.go.jp/rapdownload/), *Populus trichocarpa* (Joint Genome Initiative; http://genome.jgi-psf.org/Poptr1_1/Poptr1_1.download.ftp.html), *Vitis vinifera* (Genoscope; http://www.genoscope.cns.fr/externe/Download/Projets/Projet_ML/data/annotation/), *Selaginella moellendorffii* (http://genome.jgi-psf.org/Selmo1/Selmo1.home.html and http://genome.jgi-psf.org/Phypa1_1/Phypa1_1.home.html), and *Physcomitrella patens* (http://genome.jgi-psf.org/Phypa1_1/Phypa1_1.home.html). Homologous protein cluster data were constructed using PSI-CD-HIT of the CD-HIT program (http://cd-hit.org; Li and Godzik, 2006) with threshold of identity ≥30% and word size = 2. Other protein sequences were obtained from the National Center for Biotechnology Information database. These sequences were aligned using the ClustalX program (version 2.0.09) (Thompson et al., 1999; Larkin et al., 2007). A phylogenetic tree was constructed using MEGA version 4 (Kumar et al., 1994; Tamura et al., 2007) using the neighbor-joining method (Saitou and Nei, 1987) with Poisson correction, complete deletion, and bootstrap procedures (1000 replicates, random seed).

Expression and Purification of Recombinant UGP3 Protein

The coding sequence of *UGP3* was amplified using PCR with the primers *AT3G56040_F0* and *AT3G56040_Rnonstop* (see Supplemental Table 1 online). The sequence of UGP3-CDS disagreed with that of At3g56040 deposited in the database of TAIR, and the nucleotide substitutions result in a nonsynonymous change (*Asp530Gly*). Thus, the corresponding genomic sequence of *UGP3* of the Columbia-0 accession was confirmed using genomic PCR with *Replace check_Fw* and *Replace check_Rv* as primers. This study concluded that the 2621st and 2622nd nucleotides of the *UGP3* gene are G and A, respectively (the corresponding nucleotides are A and T on the TAIR website; see Supplemental Figure 19 and Supplemental Data Set 5 online). Thus, the amino acid at residue 530 in the polypeptide of UGP3 was determined to be Gly. The mature sequence (mUGP3-CDS) that lacks the region encoding chloroplastic transit peptides at N-terminus was amplified by PCR with the primers *AT3G56040_F(–72aa)* and *AT3G56040_Rnonstop* (see Supplemental Table 1 online for primer sequences) using UGP3-CDS as template.

The amplified DNA fragment of mUGP3-CDS was subcloned in Nova pET-53-DEST (Merck) using the TOPO directional cloning kit and LR reaction methods (Invitrogen). The plasmid, mUGP3-CDS-pET-53-DEST, was electroporated into the C41(DE3) strain of *Escherichia coli* (Avidis) carrying a chaperon plasmid pG-Tf2 (Takara Bio). The transformed *E. coli* was cultured in Luria broth supplemented with 100 μg mL^{-1} ampicillin, 20 μg mL^{-1} chloramphenicol, and 1 ng mL^{-1} tetracycline at 37°C with shaking until the OD_{600} reached ~0.4. Heterologous gene expression was then induced by treatment with 0.35 mM isopropylthio-β-galactoside followed by an overnight culture at 25°C. The cells were pelleted by centrifugation (2000*g* for 5 min) and then resuspended in 50 mM potassium phosphate, pH 7.8, containing 300 mM NaCl, 0.7% (v/v) 2-mercaptoethanol, and 0.5 mM phenylmethylsulfonyl fluoride (buffer A). The cells were disrupted by sonication, and the soluble protein fraction was recovered by collecting the supernatant after centrifugation at 14,000*g* for 10 min.

The recombinant His-tagged protein was purified using metal chelation chromatography. The soluble protein was applied to a TALON spin column (Takara Bio) equilibrated with buffer A. After washing the column with buffer A supplemented with 10 mM imidazole, proteins were eluted by increasing the concentration of imidazole to 250 mM and subjected to examination for purity and substrate specificity. The concentration of protein was determined by the method of Bradford (1976) with BSA as the standard. The kinetic constants were determined by Hanes-Woolf plot based on the Michaelis-Menten kinetics. The kinetic constant for Glc1P was determined by changing the concentration of Glc1P (0 to 10 mM) in the presence of 10 mM UTP, and that for UTP was determined by changing the concentration of UTP (0 to 10 mM) in the presence of 10 mM Glc1P.

Assay of UGPase Activity

The standard enzyme assay reaction mixture (final volume, 100 μL) consisted of 50 mM Tris-HCl, pH 7.8, 0.5 mM α-D-[1-^{13}C]glucopyranosyl-1-phosphate, 0.5 mM UTP, 10 mM $MgCl_2$, and enzyme solution. The mixture was preincubated at 30°C for 2 min, and the reaction was started by addition of substrates. After incubation for 5 min at 30°C, the reaction was stopped by adding 100 μL methanol. The supernatants of the reaction mixtures were recovered by centrifugation at 10,000*g* for 10 min. The amount of UDP-Glc in the reaction mixtures was quantified by UPLC-MS analysis. Negative ESI-MS were recorded on a Waters ZQ single quadrupole mass spectrometer. Conditions for LC were as follows: column, ACQUITY UPLC HSS T3 1.8 μm (2.1 mm i.d., 50 mm long; Waters); solvent A, water containing 5 mM dihexylammonium acetate (Tokyo Chemical Industry); solvent B, methanol containing 5 mM dihexylammonium acetate; gradient, 0 to 3.5 min, 30 to 85% B/(A + B); flow rate, 0.3 mL min^{-1}; and column temperature, 35°C. Conditions for MS were as follows: scan range, *m/z* 150 to 700; capillary voltage, 3.0 kV; cone voltage, 30 V; source temperature, 130°C; desolvation temperature, 400°C; cone gas flow, 50 $L{\cdot}h^{-1}$; desolvation gas flow, 800 $L{\cdot}h^{-1}$; nebulizer and curtain gas, N_2. For quantification of UDP-Glc, the reaction mixtures were analyzed using selected ion monitoring at *m/z* 565.05 and 566.06 for $[M–H]^-$ species of unlabeled and labeled UDP-Glc, respectively.

Transient Expression Assay in *Arabidopsis* Cells

The YFP fusion N-terminal 200 amino acids of UGP3, including cTPs, were constructed using Gateway Technology (Invitrogen). Briefly, the PCR product amplified with the primers *AT3G56040_F0* and *AT3G56040_R(200aa)* using UGP3-CDS as template was cloned into the pENTR/D-TOPO vector using the pENTR Directional TOPO Cloning Kit (Invitrogen). The entry clone and the Gateway binary vector, pH35GY, were incubated with the LR Clonase Enzyme Mix (Invitrogen) (Kubo et al., 2005). The binary plasmid was transformed to *Arabidopsis* MM1 culture cells using the *Agrobacterium tumefaciens* method. The cells that transiently expressed cTP-YFP fusion were mounted on glass slides and observed using a confocal laser scanning microscope (LSM510 META,

Axioplan2 Imaging) with a Plan-Apochromat lens (63X/1.4 oil DIC; optical slice, 1 μm) (Carl Zeiss MicroImaging). The fluorescence excited with a 488-nm laser was detected using a 505- to 530-nm band-pass for YFP and a 650-nm long-pass filter for autofluorescence. Composite figures were prepared using Zeiss LSM Image Browser software.

Transient Expression of GFP Fusion Constructs

For in situ expression of GFP fusion constructs, the full-length open reading frame of UGP3 was fused upstream and in frame of the GFP S65T gene (Chiu et al., 1996) under the control of the cauliflower mosaic virus 35S promoter. N-terminal fusion of the small subunit of ribulose-1,5-bisphosphate carboxylase/oxygenase (SSU) and SQD1 were used as controls for plastid proteins. Onion epidermal cells were bombarded with vector DNA-coated gold particles using a Bio-Rad PDS-1000He particle delivery system according to the manufacturer's instructions. After 16 h, samples were viewed using confocal laser scanning microscopy (Eclipse 80i; Nikon).

Isolation of Intact Chloroplasts

The rosette leaves of *Arabidopsis* grown on soil were digested using cell wall–digesting enzymes, and intact protoplasts were isolated according to the method of Robert et al. (2007). Intact protoplasts isolated from rosette leaves of three plants (2 g) were suspended in 5 mL of 50 mM HEPES-HCl buffer, pH 7.5, containing 0.33 M sorbitol, 1 mM $MnCl_2$, 1 mM $MgCl_2$, 2 mM EDTA, and 5 mM sodium ascorbate (buffer B). Protoplasts were disrupted by pipetting several times to release chloroplasts. Intact chloroplasts were isolated by centrifugation on a step gradient using Percoll as described by Awai et al. (2001). Intact protoplasts were washed twice with buffer B and suspended in the buffer used for assay of UGPase activity. A portion of the protoplasts was used for measurement of ADH activity, and the residual portion was used for measurement of chlorophyll content as described by Lichtenthaler (1987). ADH activity was determined as described by Dumez et al. (2006).

Analysis of UDP-Glc in *Arabidopsis* Leaves

Rosette leaves of *Arabidopsis* (250 mg fresh weight) grown in soil were frozen in liquid nitrogen and homogenized to a fine powder using a mortar and pestle. The powder was extracted with 2.5 mL of 50% (v/v) methanol and subjected to UPLC-Q-MS analysis (flow rate, 0.3 mL min^{-1}; column, ACQUITY UPLC HSS T3 1.8 μm [2.1 mm i.d., 50 mm long; Waters]; solvent, 10 mM triethylamine acetate, pH 6.0; column temperature, 30°C; conditions for MS were same as those used for assay of recombinant UGP3) (Ramm et al., 2004).

Analysis of Gene Duplication

Segmental duplication regions of the genes encoding UGPases in the *Arabidopsis*, rice, poplar, and vine grape genomes were searched for in the PGDD (http://chibba.agtec.uga.edu/duplication/). Segmental duplication regions corresponding to each *UGP3* homolog in the genomes were retrieved from the duplicated block data downloaded from PGDD with a threshold score ≥ 300.

Accession Numbers

Arabidopsis sequence data from this article can be found in the Arabidopsis Genome Initiative database under accession numbers At3g03250, At5g17310, and At3g56040. Other sequence data from this article can be found in the GenBank/EMBL data libraries under accession numbers AAY31019, CAL56361, YP_007323, ABD59006, BAD66876, XP_001690316, CAL56540, Q16222, CAL55944, XP_001692246, ABD98820, AAF62555, ABD57308, and P19595. As described in Methods, errors were found in the DNA sequence of *UGP3* deposited in the Arabidopsis Genome Initiative database. The corrected sequences of UGP3 are available in Supplemental Data Set 5 online. Other accession numbers of *Arabidopsis* genes in this article used for transcriptome analysis are as follows: At4g31780 (*MGD1*), At5g20410 (*MGD2*), At2g11810 (*MGD3*), At3g11670 (*DGD1*), At4g00550 (*DGD2*), At4g33030 (*SQD1*), At5g01220 (*SQD2*), At2g01180 (*PAP1*), At1g15080 (*PAP2*), At1g62430 (*CDS1*), and At2g39290 (*PGS1*).

Supplemental Data

The following materials are available in the online version of this article.

Supplemental Figure 1. Tissue-Specific Gene Expression Patterns of the SQDG Biosynthetic Genes in *Arabidopsis.*

Supplemental Figure 2. Induction of Expression of the SQDG Biosynthetic Genes in Wild-Type *Arabidopsis* under Phosphate Limitation.

Supplemental Figure 3. Molecular Organization of UGP3 Mutant Alleles and the Impact of Insertional Mutations on Transcript Expression.

Supplemental Figure 4. Identification of SQDG in *Arabidopsis* Leaf Lipid Extract Using Ion Trap Time-of-Flight Mass Spectrometry.

Supplemental Figure 5. LC-MS Analyses of SQDG in the Wild Type and *ugp3* Mutants.

Supplemental Figure 6. Hierarchical Clustering Analysis of Lipid Molecular Species in Wild-Type Plants and *ugp3* Mutants.

Supplemental Figure 7. LC-MS Analysis of Methanolic Extracts from the Leaves of Wild-Type Plants and *ugp3* Mutants.

Supplemental Figure 8. Sequence Alignment of *Arabidopsis* UGP3 and Homologs.

Supplemental Figure 9. Purification of UGP3 expressed in *E. coli*.

Supplemental Figure 10. Mass Spectra of Standard UDP-Glc and the Reaction Product by Recombinant UGP3.

Supplemental Figure 11. Micrographs Showing Chloroplast Targeting of UGP3.

Supplemental Figure 12. Decrease in UGPase Activity in Chloroplasts in *ugp3* Mutants.

Supplemental Figure 13. Quantification of the Transcript Level of *UGP3* in the Wild Type under Phosphate- and Sulfate-Depleted Conditions.

Supplemental Figure 14. Syntenic Relationships among the *UGP3* Homologs in Plants.

Supplemental Figure 15. Putative *UGP3* Homolog in *Physcomitrella patens*.

Supplemental Figure 16. Evolutional Studies of the UGP3 Homologs in Plants.

Supplemental Figure 17. Evolutional Studies of Type A UGPase Homologs in Higher Plants.

Supplemental Figure 18. Changes in Expression Levels of *SQD1*, *SQD2*, and *UGP3* under Sulfur Starvation Conditions.

Supplemental Figure 19. Partial Genomic Sequence of *UGP3*.

Supplemental Table 1. Primers Used in This Study.

Supplemental Data Set 1. Text File of Alignment Corresponding to Figure 4.

Supplemental Data Set 2. Text File of Alignment Corresponding to Figure 8 and Supplemental Figure 16.

Supplemental Data Set 3. Text File of Alignment Corresponding to Supplemental Figure 8.

Supplemental Data Set 4. Text File of Alignment Corresponding to Supplemental Figure 17.

Supplemental Data Set 5. Partial Genomic Sequence of *Arabidopsis UGP3* (At3g56040) and Corrected Sequences of Corresponding Genome, cDNA, and Amino Acids.

Supplemental References.

ACKNOWLEDGMENTS

We thank Y. Noutoshi (RIKEN Plant Science Center) for providing *Arabidopsis* MM1 cells and helpful suggestions. We also thank Y. Niwa (University of Shizuoka) for providing the GFP vectors, M. Araki and S. Oyama (RIKEN Plant Science Center) for their contribution to the DNA sequencing, and A. Sakata, M. Suzuki, R. Klausnitzer, and Y. Kamide (RIKEN Plant Science Center) for excellent technical support. Y.O. was a postdoctoral researcher of Shimadzu Corporation. We are also grateful to Shimadzu Corporation for their support for mass spectrometry. This work was supported in part by Grants-in-Aid from the Ministry of Education, Science, Culture, Sports, and Technology of Japan.

Received October 20, 2008; revised February 9, 2009; accepted February 19, 2009; published March 13, 2009.

REFERENCES

Akiyama, K., Chikayama, E., Yuasa, H., Shimada, Y., Tohge, T., Shinozaki, K., Hirai, Y.M., Sakurai, T., Kikuchi, J., and Saito, K. (2008). PRIMe: A Web site that assembles tools for metabolomics and transcriptomics. In Silico Biol. **8:** 339–345.

Alonso, J.M., et al. (2003). Genome-wide insertional mutagenesis of *Arabidopsis thaliana.* Science **301:** 653–657.

Awai, K., Maréchal, E., Block, M.A., Brun, D., Masuda, T., Shimada, H., Takamiya, K., Ohta, H., and Joyard, J. (2001). Two types of MGDG synthase genes, found widely in both 16:3 and 18:3 plants, differentially mediate galactolipid syntheses in photosynthetic and nonphotosynthetic tissues in *Arabidopsis thaliana.* Proc. Natl. Acad. Sci. USA **98:** 10960–10965.

Balázsi, G., Barabási, A.L., and Oltvai, Z.N. (2005). Topological units of environmental signal processing in the transcriptional regulatory network of *Escherichia coli.* Proc. Natl. Acad. Sci. USA **102:** 7841–7846.

Benning, C. (2007). Questions remaining in sulfolipid biosynthesis: A historical perspective. Photosynth. Res. **92:** 199–203.

Benning, C., Beatty, J.T., Prince, R.C., and Somerville, C.R. (1993). The sulfolipid sulfoquinovosyldiacylglycerol is not required for photosynthetic electron transport in *Rhodobacter sphaeroides* but enhances growth under phosphate limitation. Proc. Natl. Acad. Sci. USA **90:** 1561–1565.

Benning, C., and Ohta, H. (2005). Three enzyme systems for galactoglycerolipid biosynthesis are coordinately regulated in plants. J. Biol. Chem. **280:** 2397–2400.

Bird, I.F., Porter, H.K., and Stocking, C.R. (1965). Intracellular localization of enzyme associated with sucrose synthesis in leaves. Biochim. Biophys. Acta **100:** 366–375.

Bligh, E.G., and Dyer, W.J. (1959). A rapid method of total lipid extraction and purification. Can. J. Biochem. Physiol. **37:** 911–917.

Bligny, R., Gardestrom, P., Roby, C., and Douce, R. (1990). 31P NMR studies of spinach leaves and their chloroplasts. J. Biol. Chem. **265:** 1319–1326.

Bradford, M.M. (1976). A rapid and sensitive method for the quantitation of microgram quantities of protein utilizing the principle of protein-dye binding. Anal. Biochem. **72:** 248–254.

Chang, C.W., Moseley, J.L., Wykoff, D., and Grossman, A.R. (2005). The *LPB1* gene is important for acclimation of *Chlamydomonas reinhardtii* to phosphorus and sulfur deprivation. Plant Physiol. **138:** 319–329.

Chiu, W., Niwa, Y., Zeng, W., Hirano, T., Kobayashi, H., and Sheen, J. (1996). Engineered GFP as a vital reporter in plants. Curr. Biol. **6:** 325–330.

Ciereszko, I., Johansson, H., Hurry, V., and Kleczkowski, L.A. (2001). Phosphate status affects the gene expression, protein content and enzymatic activity of UDP-glucose pyrophosphorylase in wild-type and *pho* mutants of *Arabidopsis.* Planta **212:** 598–605.

Dumez, S., Wattebled, F., Dauvillee, D., Delvalle, D., Planchot, V., Ball, S.G., and D'Hulst, C. (2006). Mutants of *Arabidopsis* lacking starch branching enzyme II substitute plastidial starch synthesis by cytoplasmic maltose accumulation. Plant Cell **18:** 2694–2709.

Emanuelsson, O., Nielsen, H., and von Heijne, G. (1999). ChloroP, a neural network-based method for predicting chloroplast transit peptides and their cleavage sites. Protein Sci. **8:** 978–984.

Essigmann, B., Güler, S., Narang, R.A., Linke, D., and Benning, C. (1998). Phosphate availability affects the thylakoid lipid composition and the expression of *SQD1*, a gene required for sulfolipid biosynthesis in *Arabidopsis thaliana.* Proc. Natl. Acad. Sci. USA **95:** 1950–1955.

Essigmann, B., Hespenheide, B.M., Kuhn, L.A., and Benning, C. (1999). Prediction of the active-site structure and NAD(+) binding in SQD1, a protein essential for sulfolipid biosynthesis in *Arabidopsis.* Arch. Biochem. Biophys. **369:** 30–41.

Güler, S., Seeliger, A., Härtel, H., Renger, G., and Benning, C. (1996). A null mutant of *Synechococcus* sp. PCC7942 deficient in the sulfolipid sulfoquinovosyl diacylglycerol. J. Biol. Chem. **271:** 7501–7507.

Haas, R., Siebertz, H.P., Wrage, K., and Heinz, E. (1980). Localization of sulfolipid labeling within cells and chloroplasts. Planta **148:** 238–244.

Haines, T.H. (1973). Sulfolipids and halosulfolipids. In Lipids and Biomembranes of Eucaryotic Microorganisms, J.A. Erwin, ed (New York: Academic Press), pp. 197–232.

Härtel, H., Dörmann, P., and Benning, C. (2000). DGD1-independent biosynthesis of extraplastidic galactolipids after phosphate deprivation in *Arabidopsis.* Proc. Natl. Acad. Sci. USA **97:** 10649–10654.

Heinz, E., Schmidt, H., Hoch, M., Jung, K.H., Binder, H., and Schmidt, R.R. (1989). Synthesis of different nucleoside 5-diphospho-sulfoquinovoses and their use for studies on sulfolipid biosynthesis in chloroplasts. Eur. J. Biochem. **184:** 445–453.

Hirai, M.Y., et al. (2007). Omics-based identification of *Arabidopsis* Myb transcription factors regulating aliphatic glucosinolate biosynthesis. Proc. Natl. Acad. Sci. USA **104:** 6478–6483.

Horn, M., et al. (2004). Illuminating the evolutionary history of chlamydiae. Science **304:** 728–730.

Ihmels, J., Levy, R., and Barkai, N. (2004). Principles of transcriptional control in the metabolic network of *Saccharomyces cerevisiae.* Nat. Biotechnol. **22:** 86–92.

Joyard, J., Blee, E., and Douce, R. (1986). Sulfolipid synthesis from $^{35}SO_4$ and [1-^{14}C]acetate in isolated intact spinach chloroplasts. Biochim. Biophys. Acta **879:** 78–87.

Kleczkowski, L.A., Geisler, M., Ciereszko, I., and Johansson, H. (2004). UDP-glucose pyrophosphorylase. An old protein with new tricks. Plant Physiol. **134:** 912–918.

Kleppinger-Sparace, K.F., and Mudd, J.B. (1987). Biosynthesis of sulfoquinovosyldiacylglycerol in higher plants: The incorporation of $^{35}SO_4$ by intact chloroplasts in darkness. Plant Physiol. **84:** 682–687.

Kleppinger-Sparace, K.F., and Mudd, J.B. (1990). Biosynthesis of sulfoquinovosyldiacylglycerol in higher plants: Use of adenosine-5′-phosphosulfate and adenosine-3′-phosphate 5′-phosphosulfate as precursors. Plant Physiol. **93:** 256–263.

Kleppinger-Sparace, K.F., Mudd, J.B., and Bishop, D.G. (1985). Biosynthesis of sulfoquinovosyldiacylglycerol in higher plants: the incorporation of $^{35}SO_4$ by intact chloroplasts. Arch. Biochem. Biophys. **240:** 859–865.

Knappe, S., Flügge, U.I., and Fischer, K. (2003). Analysis of the plastidic phosphate translocator gene family in Arabidopsis and identification of new phosphate translocator-homologous transporters, classified by their putative substrate-binding site. Plant Physiol. **131:** 1178–1190.

Kobayashi, K., Awai, K., Takamiya, K., and Ohta, H. (2004). Arabidopsis type B monogalactosyldiacylglycerol synthase genes are expressed during pollen tube growth and induced by phosphate starvation. Plant Physiol. **134:** 640–648.

Kobayashi, K., Kondo, M., Fukuda, H., Nishimura, M., and Ohta, H. (2007). Galactolipid synthesis in chloroplast inner envelope is essential for proper thylakoid biogenesis, photosynthesis, and embryogenesis. Proc. Natl. Acad. Sci. USA **104:** 17216–17221.

Kobayashi, K., Masuda, T., Takamiya, K., and Ohta, H. (2006). Membrane lipid alteration during phosphate starvation is regulated by phosphate signaling and auxin/cytokinin cross-talk. Plant J. **47:** 238–248.

Kotake, T., Hojo, S., Yamaguchi, D., Aohara, T., Konishi, T., and Tsumuraya, Y. (2007). Properties and physiological functions of UDP-sugar pyrophosphorylase in *Arabidopsis.* Biosci. Biotechnol. Biochem. **71:** 761–771.

Kotake, T., Yamaguchi, D., Ohzono, H., Hojo, S., Kaneko, S., Ishida, H.K., and Tsumuraya, Y. (2004). UDP-sugar pyrophosphorylase with broad substrate specificity toward various monosaccharide 1-phosphates from pea sprouts. J. Biol. Chem. **279:** 45728–45736.

Kubo, M., Udagawa, M., Nishikubo, N., Horiguchi, G., Yamaguchi, M., Ito, J., Mimura, T., Fukuda, H., and Demura, T. (2005). Transcription switches for protoxylem and metaxylem vessel formation. Genes Dev. **19:** 1855–1860.

Kumar, S., Tamura, K., and Nei, M. (1994). MEGA: Molecular Evolutionary Genetics Analysis software for microcomputers. Comput. Appl. Biosci. **10:** 189–191.

Larkin, M.A., et al. (2007). Clustal W and Clustal X version 2.0. Bioinformatics **23:** 2947–2948.

Leustek, T., and Saito, K. (1999). Sulfate transport and assimilation in plants. Plant Physiol. **120:** 637–644.

Li, W., and Godzik, A. (2006). Cd-hit: A fast program for clustering and comparing large sets of protein or nucleotide sequences. Bioinformatics **22:** 1658–1659.

Lichtenthaler, H.K. (1987). Chlorophylls and carotenoids: Pigments of photosynthetic biomembranes. Methods Enzymol. **148:** 350–382.

Litterer, L.A., Schnurr, J.A., Plaisance, K.L., Storey, K.K., Gronwald, J.W., and Somers, D.A. (2006). Characterization and expression of Arabidopsis UDP-sugar pyrophosphorylase. Plant Physiol. Biochem. **44:** 171–180.

Maruyama-Nakashita, A., Nakamura, Y., Tohge, T., Saito, K., and Takahashi, H. (2006). Arabidopsis SLIM1 is a central transcriptional regulator of plant sulfur response and metabolism. Plant Cell **18:** 3235–3251. Figure 5(A).

Meng, M., Wilczynska, M., and Kleczkowski, L.A. (2008). Molecular and kinetic characterization of two UDP-glucose pyrophosphorylases, products of distinct genes, from *Arabidopsis.* Biochim. Biophys. Acta **1784:** 967–972.

Minoda, A., Sato, N., Nozaki, H., Okada, K., Takahashi, H., Sonoike, K., and Tsuzuki, M. (2002). Role of sulfoquinovosyl diacylglycerol for the maintenance of photosystem II in *Chlamydomonas reinhardtii.* Eur. J. Biochem. **269:** 2353–2358.

Moustafa, A., Reyes-Prieto, A., and Bhattacharya, D. (2008). Chlamydiae has contributed at least 55 genes to Plantae with predominantly plastid functions. PLoS One **3:** e2205.

Mulichak, A.M., Theisen, M.J., Essigmann, B., Benning, C., and Garavito, R.M. (1999). Crystal structure of SQD1, an enzyme involved in the biosynthesis of the plant sulfolipid headgroup donor UDP-sulfoquinovose. Proc. Natl. Acad. Sci. USA **96:** 13097–13102.

Nakano, K., Omura, Y., Tagaya, M., and Fukui, T. (1989). UDP-glucose pyrophosphorylase from potato tuber: Purification and characterization. J. Biochem. **106:** 528–532.

Nikiforova, V.J., Kopka, J., Tolstikov, V., Fiehn, O., Hopkins, L., Hawkesford, M.J., Hesse, H., and Hoefgen, R. (2005). Systems rebalancing of metabolism in response to sulfur deprivation, as revealed by metabolome analysis of Arabidopsis plants. Plant Physiol. **138:** 304–318.

Nomura, T., Nakayama, N., Murata, T., and Akazawa, T. (1967). Biosynthesis of starch in chloroplasts. Plant Physiol. **42:** 327–332.

Obayashi, T., Kinoshita, K., Nakai, K., Shibaoka, M., Hayashi, S., Saeki, M., Shibata, D., Saito, K., and Ohta, H. (2007). ATTED-II: A database of co-expressed genes and *cis* elements for identifying co-regulated gene groups in *Arabidopsis.* Nucleic Acids Res. **35:** D863–D869.

Persson, S., Wei, H., Milne, J., Page, G.P., and Somerville, C.R. (2005). Identification of genes required for cellulose synthesis by regression analysis of public microarray data sets. Proc. Natl. Acad. Sci. USA **102:** 8633–8638.

Pugh, C.E., Hawkes, T., and Harwood, J.L. (1995). Biosynthesis of sulphoquinovosyldiacylglycerol by chloroplast fractions from pea and lettuce. Phytochemistry **39:** 1071–1075.

Ramm, M., Wolfender, J.L., Queiroz, E.F., Hostettmann, K., and Hamburger, M. (2004). Rapid analysis of nucleotide-activated sugars by high-performance liquid chromatography coupled with diode-array detection, electrospray ionization mass spectrometry and nuclear magnetic resonance. J. Chromatogr. A **1034:** 139–148.

Riekhof, W.R., Ruckle, M.E., Lydic, T.A., Sears, B.B., and Benning, C. (2003). The sulfolipids 2′-*O*-acyl-sulfoquinovosyldiacylglycerol and sulfoquinovosyldiacylglycerol are absent from a *Chlamydomonas reinhardtii* mutant deleted in *SQD1.* Plant Physiol. **133:** 864–874.

Robert, S., Zouhar, J., Carter, C., and Raikhel, N. (2007). Isolation of intact vacuoles from Arabidopsis rosette leaf-derived protoplasts. Nat. Protoc. **2:** 259–262.

Roy, A.B., and Harwood, J.L. (1999). Re-evaluation of plant sulpholipid labelling from UDP-[^{14}C]glucose in pea chloroplasts. Biochem. J. **344:** 185–187.

Rudick, V.L., and Weisman, R.A. (1974). Uridine diphosphate glucose pyrophosphorylase of *Acanthamoeba castellanii*. Purification, kinetic, and developmental studies. J. Biol. Chem. **249:** 7832–7840.

Saito, K. (2004). Sulfur assimilatory metabolism. The long and smelling road. Plant Physiol. **136:** 2443–2450.

Saito, K., Hirai, M.Y., and Yonekura-Sakakibara, K. (2008). Decoding genes with coexpression networks and metabolomics – 'Majority report by precogs'. Trends Plant Sci. **13:** 36–43.

Saitou, N., and Nei, M. (1987). The neighbor-joining method: a new method for reconstructing phylogenetic trees. Mol. Biol. Evol. **4:** 406–425.

Sanda, S., Leustek, T., Theisen, M.J., Garavito, R.M., and Benning, C. (2001). Recombinant Arabidopsis SQD1 converts UDP-glucose and sulfite to the sulfolipid head group precursor UDP-sulfoquinovose *in vitro.* J. Biol. Chem. **276:** 3941–3946.

Sato, N., Sonoike, K., Tsuzuki, M., and Kawaguchi, A. (1995). Impaired photosystem II in a mutant of *Chlamydomonas reinhardtii* defective in sulfoquinovosyl diacylglycerol. Eur. J. Biochem. **234:** 16–23.

Schmid, M., Davison, T.S., Henz, S.R., Pape, U.J., Demar, M., Vingron, M., Schölkopf, B., Weigel, D., and Lohmann, J.U. (2005). A gene expression map of *Arabidopsis thaliana* development. Nat. Genet. **37:** 501–506.

Seifert, U., and Heinz, E. (1992). Enzymatic characteristics of UDP-sulfoquinovose: diacylglycerol sulfoquinovosyltransferase from chloroplast envelopes. Bot. Acta **105:** 197–205.

Shimojima, M., and Benning, C. (2003). Native uridine 5′-diphosphate-sulfoquinovose synthase, SQD1, from spinach purifies as a 250-kDa complex. Arch. Biochem. Biophys. **413:** 123–130.

Shimojima, M., Hoffmann-Benning, S., Garavito, R.M., and Benning, C. (2005). Ferredoxin-dependent glutamate synthase moonlights in plant sulfolipid biosynthesis by forming a complex with SQD1. Arch. Biochem. Biophys. **436:** 206–214.

Sugimoto, K., Sato, N., and Tsuzuki, M. (2007). Utilization of a chloroplast membrane sulfolipid as a major internal sulfur source for protein synthesis in the early phase of sulfur starvation in *Chlamydomonas reinhardtii.* FEBS Lett. **581:** 4519–4522.

Tamura, K., Dudley, J., Nei, M., and Kumar, S. (2007). MEGA4: Molecular Evolutionary Genetics Analysis (MEGA) software version 4.0. Mol. Biol. Evol. **24:** 1596–1599.

Thompson, J.D., Gibson, T.J., Plewniak, F., Jeanmougin, F., and Higgins, D.G. (1999). The CLUSTAL_X windows interface: Flexible strategies for multiple sequence alignment aided by quality analysis tools. Nucleic Acids Res. **25:** 4876–4882.

Tietje, C., and Heinz, E. (1998). Uridine-diphospho-sulfoquinovose: diacylglycerol sulfoquinovosyltransferase activity is concentrated in the inner membrane of chloroplast envelopes. Planta **206:** 72–78.

Tohge, T., et al. (2005). Functional genomics by integrated analysis of metabolome and transcriptome of *Arabidopsis* plants over-expressing an MYB transcription factor. Plant J. **42:** 218–235.

Tsuboi, K.K., Fukunaga, K., and Petricciani, J.C. (1969). Purification and specific kinetic properties of erythrocyte uridine diphosphate glucose pyrophosphorylase. J. Biol. Chem. **244:** 1008–1015.

Welti, R., Wang, X., and Williams, T.D. (2003). Electrospray ionization tandem mass spectrometry scan modes for plant chloroplast lipids. Anal. Biochem. **314:** 149–152.

Winter, D., Vinegar, B., Nahal, H., Ammar, R., Wilson, G.V., and Provart, N.J. (2007). An "electronic fluorescent pictograph" browser for exploring and analyzing large-scale biological data sets. PLoS One **2:** e718.

Xu, C., Fan, J., Froehlich, J.E., Awai, K., and Benning, C. (2005). Mutation of the TGD1 chloroplast envelope protein affects phosphatidate metabolism in *Arabidopsis.* Plant Cell **17:** 3094–3110.

Yonekura-Sakakibara, K., Tohge, T., Matsuda, F., Nakabayashi, R., Takayama, H., Niida, R., Watanabe-Takahashi, A., Inoue, E., and Saito, K. (2008). Comprehensive flavonol profiling and transcriptome coexpression analysis leading to decoding gene-metabolite correlations in *Arabidopsis.* Plant Cell **20:** 2160–2176.

Yonekura-Sakakibara, K., Tohge, T., Niida, R., and Saito, K. (2007). Identification of a flavonol 7-*O*-rhamnosyltransferase gene determining flavonoid pattern in *Arabidopsis* by transcriptome coexpression analysis and reverse genetics. J. Biol. Chem. **282:** 14932–14941.

Yu, B., Xu, C., and Benning, C. (2002). *Arabidopsis* disrupted in *SQD2* encoding sulfolipid synthase is impaired in phosphate-limited growth. Proc. Natl. Acad. Sci. USA **99:** 5732–5737.

Yu, B., Xu, C., and Benning, C. (2003). Anionic lipids are required for chloroplast structure and function in Arabidopsis. Plant J. **36:** 762–770.

Zimmermann, P., Hennig, L., and Gruissem, W. (2005). Gene expression analysis and network discovery using Genevestigator. Trends Plant Sci. **10:** 407–409.